

Central Lancashire Online Knowledge (CLoK)

Title	Resveratrol prevents brain edema, blood-brain barrier permeability, and altered aquaporin profile in autism animal model
Type	Article
URL	https://clock.uclan.ac.uk/38465/
DOI	https://doi.org/10.1002/jdn.10137
Date	2021
Citation	Deckmann, Iohanna, Santos-Terra, Júlio, Fontes-Dutra, Mellanie, Körbes-Rockenbach, Marília, Bauer-Negrini, Guilherme, Brum Schwingel, Gustavo, Riesgo, Rudimar, Bambini-Junior, Victorio and Gottfried, Carmen (2021) Resveratrol prevents brain edema, blood-brain barrier permeability, and altered aquaporin profile in autism animal model. <i>International Journal of Developmental Neuroscience</i> , 81 (7). pp. 579-604. ISSN 0736-5748
Creators	Deckmann, Iohanna, Santos-Terra, Júlio, Fontes-Dutra, Mellanie, Körbes-Rockenbach, Marília, Bauer-Negrini, Guilherme, Brum Schwingel, Gustavo, Riesgo, Rudimar, Bambini-Junior, Victorio and Gottfried, Carmen

It is advisable to refer to the publisher's version if you intend to cite from the work.
<https://doi.org/10.1002/jdn.10137>

For information about Research at UCLan please go to <http://www.uclan.ac.uk/research/>

All outputs in CLoK are protected by Intellectual Property Rights law, including Copyright law. Copyright, IPR and Moral Rights for the works on this site are retained by the individual authors and/or other copyright owners. Terms and conditions for use of this material are defined in the <http://clock.uclan.ac.uk/policies/>

Deckmann Iohanna (Orcid ID: 0000-0002-6423-1938)
Santos-Terra Júlio (Orcid ID: 0000-0002-8079-452X)
Fontes-Dutra Mellanie (Orcid ID: 0000-0003-0334-0740)
Schwingel Gustavo Brum (Orcid ID: 0000-0002-8949-6254)

**RESVERATROL PREVENTS BRAIN EDEMA, BLOOD-BRAIN BARRIER
PERMEABILITY AND ALTERED AQUAPORIN PROFILE IN AUTISM ANIMAL
MODEL**

Iohanna Deckmann^{a,b,c,d,#}, Júlio Santos-Terra^{a,b,c,d}, Mellanie Fontes-Dutra^{a,b,c,d},
Marília Körbes-Rockenbach^{a,b,c}, Guilherme Bauer-Negrini^{a,b,c,d}, Gustavo Brum
Schwingel^{a,b,c,d}, Rudimar Riesgo^{a,c,d,e}, Victorio Bambini-Junior^{a,c,d,f}, Carmem
Gottfried^{a,b,c,d}

a Translational Research Group in Autism Spectrum Disorder - GETTEA, Universidade Federal do Rio Grande do Sul (UFRGS), Porto Alegre, Brazil.

b Department of Biochemistry, Universidade Federal do Rio Grande do Sul (UFRGS), Porto Alegre, Brazil.

c National Institute of Science and Technology in Neuroimmunomodulation - INCT-NIM, Brazil.

d Autism Wellbeing and Research Development - AWARD - Initiative BR-UK-CA

e Department of Pediatrics, Child Neurology Unit, Hospital de Clínicas de Porto Alegre, Porto Alegre, Brazil.

f School of Pharmacology and Biomedical Sciences, University of Central Lancashire, Preston, UK.

#ORCID ID: 0000-0002-6423-1938

Corresponding authors:

ID (iohanna.deckmann@gmail.com) and CG (cgottfried@ufrgs.br)

Departamento de Bioquímica, ICBS, Universidade Federal do Rio Grande do Sul, Ramiro Barcelos 2600 – 21111. CEP: 90035-003 Porto Alegre-RS, Brazil.

This article has been accepted for publication and undergone full peer review but has not been through the copyediting, typesetting, pagination and proofreading process which may lead to differences between this version and the Version of Record. Please cite this article as doi: 10.1002/jdn.10137

Co-author e-mail address:

ID (iohanna.deckmann@gmail.com); JS-T (juliosterra@gmail.com); MF-D (dutra.mellanie@gmail.com); MK-R (mariliakrockenbach@gmail.com); GB-N (negrini.guilherme@gmail.com); GBS (brumschwengel@gmail.com); RR (rriesgo@hcpa.edu.br); VB-J (VBambini-Junior@uclan.ac.uk); CG (cgottfried@ufrgs.br).

Funding statement: This work was supported by Instituto Nacional de Ciência e Tecnologia em Neuroimunomodulação (INCT-NIM #465489/2014-1), Rio de Janeiro, Brazil; Conselho Nacional de Desenvolvimento Científico e Tecnológico (CNPq), Coordenação de Aperfeiçoamento de Pessoal de Nível Superior (CAPES) and Fundo de Incentivo à Pesquisa e Eventos do Hospital de Clínicas de Porto Alegre (FIPE-HCPA #13-0047). We would also like to thank Fluxome (Stenløse, Denmark) for the generous gift of *trans*-resveratrol.

Conflict of Interest: The authors declare that they have no conflict of interest.

Data availability statement: “Research data are not shared.”

Ethical statement: All procedures were approved by the local Ethics Commission on the Use of Animals (CEUA-UFRGS 36229) and performed according to ethical principles in accordance with the NIH Guide for the Care and Use of Laboratory Animals, as well as Brazilian Arouca Law (11,794, of October 8, 2008).

Author contributions: ID, JS-T, MF-D, MK-R, GB-N, GBS, RR, VB-J and CG: experimental design and intellectual contribution. RR, VB-J and CG: acquisition of financial resources. ID, GB-N and GBS: edema and Evans blue analyses. ID, JS-T, MF-D and MK-R: immunofluorescence and western blotting analyses. ID, JS-T, MF-D, VB-J and CG: data discussion and manuscript preparation.

Abbreviations: aCC: anterior cingulate cortex (in the medial prefrontal cortex); AmR: amygdala region; AQP: aquaporin; ASD: autism spectrum disorder; BBB: blood-brain barrier; CA: cornu ammonis (CA1-CA3, in the hippocampus); CNS: central nervous system; GFAP: glial fibrillary acidic protein; IL: infralimbic cortex (in

the medial prefrontal cortex); MIA: maternal immune activation; mPFC: medial prefrontal cortex;

PrL: prelimbic cortex (in the medial prefrontal cortex); pSSA: primary somatosensory area; RSV: resveratrol; VPA: valproic acid.

Highlights:

- Autism Spectrum Disorder (ASD) is hallmarked by neuroimmune background;
- ASD animal model replicates the greater brain volume described in ASD patients;
- Resveratrol (RSV) prevents blood-brain barrier alterations and edema formation;
- RSV restore AQP4 levels to control levels;
- RSV promotes a functional amelioration in astrocytes.

Abstract

Autism Spectrum Disorder can present a plethora of clinical conditions associated with the disorder, such as greater brain volume in the first years of life in a significant percentage of patients. We aimed to evaluate the brain water content, the blood-brain barrier permeability, and the expression of aquaporin 1 and 4, and GFAP in a valproic acid-animal model, assessing the effect of resveratrol. On postnatal day 30, Wistar rats of the valproic acid group showed greater permeability of the blood-brain barrier to the Evans blue dye and a higher proportion of brain water volume, prevented both by resveratrol. Prenatal exposition to valproic acid diminished aquaporin 1 in the choroid plexus, in the primary somatosensory area, in the amygdala region and in the medial prefrontal cortex, reduced aquaporin 4 in medial prefrontal cortex and increased aquaporin 4 levels in primary somatosensory area (with resveratrol prevention). Valproic acid exposition also increased the number of astrocytes and GFAP fluorescence in both primary somatosensory area and medial prefrontal cortex. In medial prefrontal cortex, resveratrol prevented the increased fluorescence. Finally, there was an effect of resveratrol *per se* on the number of astrocytes and GFAP fluorescence in the amygdala region and in the hippocampus. Thus, this work demonstrates significant changes in blood-brain barrier permeability, edema formation, distribution of aquaporin 1 and 4, in addition to astrocytes profile in

the animal model of autism, as well as the use of resveratrol as a tool to investigate the mechanisms involved in the pathophysiology of Autism Spectrum Disorder.

Keywords: Autism spectrum disorder. Valproic acid. Resveratrol. Water content. Blood-brain barrier. Aquaporin.

1. INTRODUCTION

Autism Spectrum Disorder (ASD) was first characterized in the 1920s by the Russian psychiatrist Grunya Sukharewa, who described 6 children with autistic characteristics (Ssucharewa, 1926; Zeldovich, 2018). Currently, ASD is a highly prevalent neurodevelopmental disorder characterized by 1) deficits in communication and social interaction and 2) the presence of repetitive behaviors and restricted interests/activities (APA, 2013), affecting 1:54 children up to 8 years old in the USA (Maenner et al., 2020).

Despite research advances on this disorder, the etiology of ASD remains unknown. However, epidemiological observations suggest that environmental factors, such as valproic acid (VPA), are closely related to the onset of ASD (Christensen et al., 2013; Rouillet et al., 2013; Smith & Brown, 2014). Besides the core symptoms, several conditions associated with ASD are described, including greater brain volume in the first years of life (Aylward et al., 2002) affecting around 20% of ASD patients (Sacco et al., 2015).

For a long time, it was hypothesized that the Central Nervous System (CNS) was an immunologically privileged location (Tambur & Roitberg, 2005) due to blood-brain barrier (BBB), a selective barrier composed, among others, by astrocytes (Abbott, 2013). Several studies relate astrocytic dysfunctions to psychiatric disorders, including ASD (Mony et al., 2016; Zeidán-Chuliá et al., 2014). Increased reactive gliosis, proliferation of glial cells in the brain of ASD individuals (Petrelli et al., 2016) as well as the association between ASD and genes related to the activation of glia and the immune system (Voineagu et al., 2011), stressing the role of astrocytes in ASD and in BBB impairments.

Besides astrocytes, the BBB's dynamic can be affected by the water channels aquaporins (AQP). AQP1 is expressed mainly in the apical membrane of the choroid plexus (involved in the production of cerebrospinal fluid), in addition to glial membranes, astrocytes and ependymal cells (Benga & Huber, 2012; Oshio et al., 2003). On the other hand, AQP4 is the most common water channel in the CNS,

present in greater quantity in terminal feet of astrocytes that surround blood vessels (essential constituent of BBB) (Nagelhus & Ottersen, 2013; Papadopoulos & Verkman, 2007; Xiao & Hu, 2014), playing an important role in removing water from the cerebral parenchyma, in addition to assisting the potassium buffering (Benga & Huber, 2012).

Few studies have been conducted related to BBB and AQP alteration in ASD individuals, indicating decreased cerebellar AQP4 (*postmortem*) (Fatemi et al., 2008), and no alteration in serum (Kalra et al., 2015), as well as a huge cerebellar permeability in the VPA-animal model of ASD (Kumar & Sharma, 2016b, 2016a; Kumar et al., 2015). Considering the increased brain volume and the possible impairment of neural barrier systems, as well as the pro-inflammatory and pro-oxidant processes already observed in ASD individuals, molecules with antioxidant and anti-inflammatory properties become important targets for the study of neuroprotective mechanisms in ASD.

The *trans*-resveratrol (RSV, 3,5,4'-trihydroxystilbene) is a naturally occurring polyphenolic compound present in grapes, peanuts and red wine, having several biological effects (Frémont, 2000; Vang et al., 2011). Several studies emphasizing the protective and therapeutic roles of RSV in several pathologies (Berman et al., 2017; Koushki et al., 2020), highlighting the anti-inflammatory (J.-A. Lee et al., 2015; Sánchez-Fidalgo et al., 2010), antioxidant (Mohammadshahi et al., 2014) and neuroprotective effects (Quincozes-Santos & Gottfried, 2011; Tang, 2010) of RSV.

Our research group have been demonstrated the preventive effect of prenatal treatment with RSV in sociability and sensory deficits in the offspring of VPA-animal model (Bambini-Junior et al., 2014; Fontes-Dutra et al., 2018), as well as in microRNA levels (Hirsch et al., 2018). These results enable the use of RSV as both a reliable method for understanding the pathophysiology of ASD and an assisting tool in the study of biological routes and structures involved in its etiology.

The mechanisms that mediate the brain volume dynamics are largely unknown; thus, we proposed an investigation of factors possibly associated with the formation of brain edema in ASD in an animal model of autism. Thus, we aimed to evaluate the proportion of brain fluid volume, the BBB permeability, as well as to analyze AQP 1 and 4 and GFAP+-astrocytes in 30-day-old animals of the animal model of autism induced by prenatal exposure to VPA, evaluating the possible therapeutic effect of RSV.

2. EXPERIMENTAL PROCEDURE

2.1 Animals

Wistar rats from the Center for Reproduction and Experimentation of Laboratory Animals (CREAL-UFRGS) of the Federal University of Rio Grande do Sul (UFRGS) were used, kept in standard animal facilities conditions, with food and water *ad libitum*, light/dark cycle 12 hours, constant temperature ($22^{\circ}\text{C} \pm 1^{\circ}\text{C}$) and a maximum of four animals per housing box. All procedures were approved by the local Ethics Commission on the Use of Animals (CEUA-UFRGS 36229) and performed according to ethical principles in accordance with the NIH Guide for the Care and Use of Laboratory Animals, as well as Brazilian Arouca Law (11,794, of October 8, 2008).

The animals' euthanasia procedure followed the Euthanasia Practice Guidelines of the National Council for Animal Experimentation Control (Normative Resolution N. 13, 2013). Euthanasia was performed by anesthetic overdose with ketamine and xilasine, supplied in concentrations three times higher (300 mg/kg and 40 mg/kg, respectively) than the concentration required to obtain an anesthetic-surgical plan.

2.2 Animal model and RSV treatment

The animals were mated overnight and, in the next morning, the presence of sperm was verified in the vaginal canal of the females; when fertilization was confirmed, the embryonic day 0.5 (E0.5) was determined. From E6.5 to E18.5, pregnant rats received RSV (trans-resveratrol, Fluxome, Stenløse, Denmark - 3.6 mg/kg) or dimethylsulfoxide (DMSO P.A. - vehicle, equivalent volume of RSV injection in a proportion 1:1 of DMSO and saline) subcutaneously. At E12.5, pregnant rats received a single injection of VPA (sodium valproate, Sigma-Aldrich, USA - 600mg/kg) or saline solution (0.9% - vehicle) via intraperitoneal (i.p.), as previously described (Bambini-Junior et al., 2014). On postnatal day 21 (P21), the litter was weaned and, at P30, male rats were euthanized by anesthetic overdose. The total number of animals used in the study was 24 control, 28 RSV, 25 VPA, and 22 RSV+VPA divided randomly among experiments, generated from the following number of dams: 5 control, 7 RSV, 14 VPA, and 12 RSV+VPA. As we use a maximum of 1 male from the same litter in each group, the excess offspring per litter was destined to other projects in the lab). The litters were randomly divided so that sibling animals were not part of

the same experiment (n of animals is n of litters). The loss rate for the VPA groups was 50% in this protocol.

2.3 Tissue preparation and analysis

2.3.1 Brain water content

Immediately after the euthanasia, the brains were removed, weighed, and placed in a drying oven at 60°C. After 72h, brains were reweighed and the brain water content was measured considering the difference between wet tissue weight (w) and dry weight (d) (Wei et al., 2015). We considered the animal body weight since the animals prenatally VPA-exposed presented lower body weight throughout the development as described by Schneider et al., 2005 (Schneider & Przewłocki, 2005) as follows: $\{[(\text{wet weight} - \text{dry weight})/\text{wet weight}] \times 100/\text{animal body weight}\}$.

2.3.2 Evans blue dye permeability

The animals were injected via i.p. with Evans blue 2% solution (4 mg/kg) diluted in saline solution 0,9% (Kumar et al., 2015) and, after 2 hours, were anesthetized and subjected to transcardiac perfusion with saline solution and 4% paraformaldehyde. The brain was removed, post-fixed in 4% paraformaldehyde and preserved in sucrose (15% and 30%). The tissues were kept in an ultrafreezer (-80°C) until coronal slices (25 µm) were made in cryostat (Leica Microsystems). The brain coordinates following Paxinos Atlas (5th edition): bregma 3.72/3.24 (medial prefrontal cortex - mPFC) and -2.92/-3.00 (primary somatosensory area - pSSA, amygdala region - AmR, hippocampus and choroid plexus).

The slices were also incubated with DAPI solution for marking nuclei (diluted in 1:10,000 in saline solution 0.9%) for 10 minutes, followed by 5 washes with 0.1 M pH 7.4 PBS (3 minutes each) and adding the Fluoshield® mounting medium and the coverslip. The images were obtained in a 20x magnification using a confocal microscope (Olympus FV1000 – Olympus FluoView 4.0 Viewer) at the Center for Microscopy and Microanalysis (CMM-UFRGS) and the fluorescence was analyzed using the ImageJ® software.

2.3.3 Immunofluorescence

After anesthesia, the animals were euthanized by transcardiac perfusion with saline solution 0.9% and 4% paraformaldehyde, the brain was removed, preserved and cut as already described.

The technique was performed according to a previous protocol (Fontes-Dutra et al., 2018) and followed the following steps: 1) tissue permeabilization with PBS-Triton 0.1% or 0.3% (according to primary antibody); 2) 3 washes with PBS; 3) blocking with PBS-Triton 0.1% (or 0.3%) containing 5% bovine serum albumin (BSA); 4) incubation with primary antibodies for 48h at 4°C in PBS-Triton 0.1% (or 0.3%) BSA 1% solution; 5) 5 washes with PBS buffer; 6) incubation with secondary antibodies for 2 hours at room temperature; 7) 5 washes with PBS; 8) incubation with DAPI solution (1:10,000 - 10 minutes); 9) 5 washes with PBS followed by addition of Fluoshield® mounting medium and coverslip. The images were obtained as previously described. Two trained researchers did manual analysis of both fluorescence distribution and cell counting in the brain regions and subregions, blinded for the experimental groups, using the ImageJ® software.

All primary antibodies were chosen according to the previous data from references cited in the manufacturer datasheets. All reagent information were detailed in Supplementary Table 1. Representative images of the AQP1 and AQP4 labeling can be seen in Supplementary Figure 1 and Supplementary Figure 2, respectively.

2.3.4 Western blotting

Following to the euthanasia, the brain was removed and the mPFC, pSSA, AmR and hippocampus were dissected.

The samples were homogenized in a buffer containing protease inhibitor, 10% SDS, EDTA 100 mM, TRIS/HCl buffer 500 mM pH 8. The total proteins were quantified by the Lowry method (Lowry et al., 1951) and the samples prepared in a buffer containing glycerol, bromophenol blue, TRIS/HCl buffer and β -mercaptoethanol. 40 μ g of protein was applied in 10% polyacrylamide gel, separated by one-dimensional electrophoresis and transferred to nitrocellulose membranes for the detection of the AQP1 and AQP4 immunocontents. The membranes were blocked in 5% BSA dissolved in a pH 7.5 TRIS buffer (TBS) with 0.1% Tween-20 (TTBS) and incubated overnight at 4°C with the primary antibodies.

After incubation, the membranes were washed with TTBS and incubated with secondary antibodies, followed by 3 washes. The substrate SuperSignal® West Pico (Thermo Fisher Scientific) was used on the membranes and the chemiluminescent signal was detected using ImageQuant™ LAS 4000 (GE HealthCare Life Sciences). The quantification of the relative immunocontent was performed with the ImageJ software (v. 1.51) and the data was normalized by the housekeeping protein β -actin. All reagent information were detailed in Supplementary Table 1.

2.4 Statistical analysis

The data were analyzed using the IBM SPSS Statistics 20 program (IBM SPSS, Armonk, NY, USA). Kolmogorov-Smirnov and Shapiro-Wilk tests of normality were applied to determine data distribution. The data of "edema" and "BBB permeability to Evans blue dye" had a non-normal distribution; therefore, a non-parametric test was performed for independent samples (Kruskal-Wallis). Immunofluorescence and western blotting data showed normal data distribution, using the two-way ANOVA test followed by Sidak's post-test. When there was an interaction effect, pairwise comparison was analyzed in the post hoc; when there was no effect, the effect of exposure to factors (VPA or RSV) was analyzed.

The graphs were made using the GraphPad Prism 6 program. Data were reported as median \pm interquartile range (IQR) for the non-parametric test and mean \pm standard deviation for the parametric test. $p < 0.05$ was considered statistically significant.

3. RESULTS

3.1. Prenatal administration of RSV prevents the alterations induced by prenatal exposure to VPA in body weight and in proportional brain water content at P30

Prenatal exposure to VPA increased brain water content ($p = 0.003$, Figure 1A), decreased body weight ($p = 0.001$, Figure 1B) and increased proportion of brain fluid ($p = 0.002$, Figure 1C). In this experiment, prenatal treatment with RSV was able to prevent these alterations. Detailed statistics are shown in Table 1.

3.2. Prenatal administration of RSV prevents the increased BBB permeability induced by VPA at P30

The VPA group had increased BBB permeability to Evans blue dye (representative images in Figure 2) in the choroid plexus ($p = 0.009$), in the pSSA, both in layers II/III ($p = 0.004$) and IV/V ($p = 0.005$), in subregions of the mPFC when compared to the control and/or RSV group) anterior cingulate cortex (aCC) (II/III: $p = 0.001$; IV/V: $p = 0.013$); 2) prelimbic cortex (PrL) (II/III: $p = 0.019$; IV/V: $p = 0.022$); and 3) infralimbic cortex (IL) (II/III: $p = 0.028$; IV/V: $p = 0.016$). RSV was able to prevent the permeability alterations in these regions. No significant difference was observed in dye permeability in the hippocampus ($p = 0.134$) or in the AmR ($p = 0.050$). Detailed statistics are shown in Table 2.

3.3. Prenatal exposure to VPA changes choroid plexus morphology and decreases AQP1 distribution at P30

The choroid plexus from both groups exposed to VPA had a huge morphological alteration (indicated by the white arrow in Figure 3A) and decreased AQP1 labeling (Figure 3A-3B, control: 1244 ± 279.3 ; RSV: 1053 ± 131.9 ; VPA: 867.1 ± 76.11 ; RSV+VPA: 798.6 ± 221.3 ; $F(3, 16) = 5.345$, $p_{\text{VPA}} = 0.0022$). These alterations were not prevented by RSV.

3.4. Prenatal administration of RSV prevents the VPA-induced increase in AQP4-immunocontent and distribution in pSSA at P30.

Prenatal exposure to VPA decreased AQP1 content in pSSA (Figure 4A, Control: 1.594 ± 0.073 ; RSV: 1.342 ± 0.210 ; VPA: 1.148 ± 0.180 ; RSV+VPA: 0.834 ± 0.185 ; $F(1, 12) = 31.39$; $p_{\text{VPA}} = 0.0001$) in deep layers (II/III: $p_{\text{interaction}} = 0.9098$; IV/V: $p_{\text{VPA}} = 0.0005$) with no preventive effect by RSV (Table 3). Interestingly, the VPA group had increased AQP4 content in pSSA (Figure 4E, control: 1.445 ± 0.0256 ; RSV: 1.086 ± 0.149 ; VPA: 2.391 ± 0.368 ; RSV+VPA: 1.457 ± 0.314 ; $F(1, 12) = 5.128$; $p_{\text{interaction}} = 0.0429$) in deep layers (II/III: $p_{\text{interaction}} = 0.4255$; IV/V: $p_{\text{interaction}} = 0.0011$) with a significant preventive effect of RSV. Detailed statistics of immunofluorescence are shown in Table 3.

3.5. mPFC has decreased levels of both AQP1 and AQP4 induced by prenatal exposure to VPA

Despite no change was observed in the AQP1 immunocontent in mPFC from VPA group (Figure 4C, control: 1.221 ± 0.185 ; RSV: 1.124 ± 0.182 ; VPA: 1.081 ± 0.389 ; RSV+VPA: 0.975 ± 0.195 ; $F(1, 12) = 0.00095$; p interaction = 0.9759), both groups exposed prenatally to VPA presented decreased distribution of this protein in all subregions of the mPFC, with no preventive effect of RSV: aCC – layers II/III (p VPA = 0.0043) and IV/V (p VPA = 0.0010); PrL – layers II/III (p VPA = 0.0010) and IV/V (p VPA < 0.0001); IL – layers II/III (p VPA = 0.0009) and IV/V (p VPA = 0.0004) (Table 4).

The VPA group had decreased content of AQP4 (Figure 4G, control: 0.816 ± 0.196 ; RSV: 1.019 ± 0.130 ; VPA: 0.387 ± 0.164 ; RSV+VPA: 0.946 ± 0.507 ; $F(1, 12) = 6.808$; p RSV = 0.0228) with decreased distribution of this protein in all subregions of the mPFC: aCC – layers II/III (p interaction = 0.0421) and IV/V (p interaction = 0.0125); PrL – layers II/III (p interaction = 0.0449) and IV/V (p interaction = 0.0167); IL – layers II/III (p interaction = 0.0412) and IV/V (p interaction = 0.0171). Detailed statistics of immunofluorescence are shown in Table 4.

3.6. Intrauterine exposure to VPA induces a decrease in AQP1 in the AmR

Despite no differences were observed in AQP1 immunocontent in the AmR among experimental groups (Figure 4B, Control: 0.918 ± 0.214 ; RSV: 1.089 ± 0.399 ; VPA: 0.871 ± 0.113 ; RSV+VPA: 0.842 ± 0.277 ; $F(1, 12) = 0.6424$; p interaction = 0.4384), both groups that received VPA had decreased distribution of AQP1 (p VPA = 0.0004) (Table 5). No changes were observed in both AQP4 content (Figure 4F, Control: 1.192 ± 0.457 ; RSV: 1.288 ± 0.333 ; VPA: 0.943 ± 0.108 ; RSV+VPA: 1.512 ± 0.521 ; $F(1, 12) = 1.484$; p interaction = 0.2466) and in distribution among groups (p interaction = 0.5988). Detailed statistics of immunofluorescence are shown in Table 5.

3.7. Prenatal exposure to VPA does not alter the expression profile of AQP1 and AQP4 in the hippocampus, but the RSV treatment had a *per se* effect

No changes were observed in the hippocampal content of AQP1 (Figure 4D, Control: 1.031 ± 0.275 ; RSV: 0.927 ± 0.273 ; VPA: 0.941 ± 0.214 ; RSV+VPA: 0.977 ± 0.238 ; $F(1, 12) = 0.3097$; p interaction = 0.5881). However, a *per se* effect of

RSV was observed, with decreased AQP1 distribution in dentate gyrus and CA2 region: Dentate gyrus (p RSV = 0.0412); CA1 (p RSV = 0.0518); CA2 (p RSV = 0.0330); CA3 (p RSV = 0.0810) (Table 6).

No changes were observed in both AQP4 content (Figure 4H, Control: 0.533 ± 0.271 ; RSV: 0.422 ± 0.221 ; VPA: 0.291 ± 0.106 ; RSV+VPA: 0.360 ± 0.116 ; $F(1, 12) = 0.8866$; p interaction = 0.365) and distribution among groups: dentate gyrus (p interaction = 0.0387); CA1 (p interaction = 0.0786); CA2 (p interaction = 0.1113); CA3 (p interaction = 0.0490). Detailed statistics of immunofluorescence are shown in Table 6.

3.8 RSV treatment improves the functional but not morphological aspect of astrocytic changes induced by prenatal exposure to VPA

3.8.1 Primary somatosensory area

An increased number of GFAP⁺-astrocytes was observed in layers II/III (p VPA = 0.0038) and in layers IV/V (p VPA = 0.0038) in both groups that were prenatally exposed to VPA (representative image in Figure 5). As expected, this data was reflected by increased GFAP immunofluorescence per area (II/III: p VPA = 0.0270; IV/V: p RSV = 0.0380). Detailed statistics are shown in Table 7.

3.8.2 Medial prefrontal cortex

This region showed different effects between the upper (II/III) and deeper (IV/V) layers. In upper layers, exposition to VPA increases the number of astrocytes, with no preventive effect of RSV (aCC: p VPA = 0.0135; PrL: p VPA = 0.0269; IL: p VPA = 0.0278), which was reflected in the GFAP immunofluorescence values (aCC: p VPA = 0.0379; PrL: p VPA = 0.0604; IL: p interaction = 0.5621).

In deeper layers, both groups exposed to VPA increased the number of GFAP⁺-astrocytes (aCC: p VPA = 0.0091; PrL: p VPA = 0.0004; IL: p VPA = 0.0018). However, we observed increased GFAP immunofluorescence in the VPA group, with a significantly preventive effect of RSV (aCC: p interaction = 0.0171; PrL: p interaction = 0.2853; IL: p interaction = 0.0455). Detailed statistics are shown in Table 8.

3.8.3 Amygdala region

In this region, we observed a *per se* effect of RSV, with decreased number GFAP⁺-astrocytes (p interaction = 0.0017) and GFAP immunofluorescence (p interaction = 0.0450) in RSV group. Detailed statistics are shown in Table 9.

3.8.4 Hippocampus

Another *per se* effect of RSV was observed in number of GFAP⁺-astrocytes (dentate gyrus: p interaction = 0.0162; CA1: p interaction = 0.1926; CA2: p RSV = 0.0001; CA3: p interaction = 0.0461) and GFAP immunofluorescence values (dentate gyrus: p interaction = 0.0096; CA1: p interaction = 0.0172; CA2: p interaction = 0.0214; CA3: p interaction = 0.0058). Detailed statistics are shown in Table 10.

4. DISCUSSION

A significant percentage of ASD patients presents increased brain volume in the first years of life, followed by an apparent normalization of this volume in late childhood (Aylward et al., 2002; Bartholomeusz et al., 2002; Emerson et al., 2017; Hazlett et al., 2011). Recent evidence in animal models has been highlighting the association of maternal inflammatory processes during critical embryonic development with excessive brain growth and with the triggering of ASD-associated behavior in the offspring (Le Belle et al., 2014). In fact, maternal immune activation (MIA) contributes to the onset of several neuropsychiatric disorders, including ASD (Estes & McAllister, 2016). Thus, we postulate that the fingerprint caused by prenatal exposure to VPA could involve mechanisms of MIA since animals from VPA-animal model present enhanced levels of IL-1 β , IL-6, and TFN- α in the hippocampus and other brain regions (Deckmann et al., 2018), besides enhanced TFN- α levels and microglial activation after prenatal VPA exposure (Zamberletti et al., 2019).

In the present study, we demonstrated that the prenatal exposure to VPA increased the absolute brain water content, providing a clearer overview of the higher liquid volume in the brain of the VPA group even though the body structure was smaller. The preventive effect of RSV against these changes, in addition to the alterations in the proteins AQP1 and AQP4 according to brain region, opens new clues about the mechanisms associated to the brain volume changes in ASD patients.

The VPA group presented evident BBB permeability in brain regions related to the neocortex: choroid plexus (directly in contact with neocortex), pSSA (layers II/III

and IV/V) and all subregions of the mPFC (aCC, PrL and IL, in superficial and deeper layers). In all of these regions, RSV treatment was able to prevent the BBB permeability. BBB damage can be a pivotal event for brain edema development, which could be both initiated and regulated by several pro-inflammatory mediators (among them cytokines and chemokines) that coordinate the extent of leukocyte entry to the brain parenchyma, causing loosening of the tight junctions and vasogenic edema (Stamatovic et al., 2006). RSV, known by its antioxidants and anti-inflammatory properties, could be acting as a neuroprotective molecule in different pathways during embryonic development. In a model of cerebral ischemia-reperfusion, RSV attenuates BBB dysfunctions and reverses the brain water accumulation by the regulation of matrix metalloproteinase 9 (MMP-9) (Wei et al., 2015). MMP-9 is an enzyme with zinc-dependent proteolytic activity that has the ability to break down collagen IV (which composes basal lamina) and whose increased levels were associated with neurodevelopmental disorders, including ASD (Reinhard et al., 2015). Both VPA and RSV are able to act in an epigenetic way, mainly modulating the histone activity. The histone deacetylase inhibition (HDACi) - an effect of VPA - is able to induce several effects on the BBB stabilization by the deregulation of important transcription factors associated with BBB formation like SOX7, SOX18, TAL1, and ETS1 (Roudnicky et al., 2020), as well as is known to interfere in the immune system, inducing increased transcription of proinflammatory genes associated with the NFkappaB pathway, for example (Rahman et al., 2004). This is important since inflammatory mediators are known to increase the BBB permeability, leading to an inflammatory infiltrate in the CNS, and are associated with neurodevelopmental disorders, such as ASD. Complementary, VPA-prenatal exposure promotes systemic inflammation, and is known that the maternal immune activation (MIA) animal model is associated with BBB disruption (Simões et al., 2018). The early treatment with RSV (beginning at E6.5) probably reduced BBB alterations by the attenuating HDACi induced by VPA through the activating Sirt and promoting modulations of proteins like MMP9 and TIMP1 (Moussa et al., 2017; Sawda et al., 2017; Wei et al., 2015). Therefore, RSV acts as a stabilizer of the transcription, preventing both BBB cell alterations (directly) and the shift for a proinflammatory status in the immune system (indirectly).

We investigated the expression and distribution of aquaporins, important water channels, in different regions of CNS. These proteins perform several roles, but one of the main ones is to facilitate the movement of water, both in and out of the CNS

(Rosu et al., 2019). The VPA group decreased the AQP1 distribution in the choroid plexus, in the deeper layers of pSSA, in the AmR and in all of the subregions of mPFC analyzed. Choroid plexus is crucial given its role in the production and release of CSF and it has been shown that in animals knocked out for AQP1 there was a reduction of up to 25% in the rate of cerebrospinal fluid secretion (Oshio et al., 2003). In addition, a morphological alteration was observed in the insertion of the choroid plexus in the third ventricle. A similar lesion was observed in a model of cerebral ischemic edema (Akdemir et al., 2016), but here in the present study, we do not consider any association between this morphological alteration and the pathophysiology of ASD, which may simply be a teratogenic effect of VPA *per se*.

The VPA group increased the AQP4 content in deeper layers of the pSSA (prevented by RSV) whereas the mPFC presented decreased levels without prevention by the RSV. Alterations on the AQP4 profile in *postmortem* brain tissue of ASD individuals have already been reported (Fatemi et al., 2008), including a discrete reduction in Brodmann area 9 (BA9 - equivalent of the frontal cortex) and an increase in the BA40 (parietal cortex, where is the pSSA). They also showed increased connexin 43 levels (a protein present in astrocytic gap junction) in BA9, representing an increase in neuroglial signaling and an improvement of cell-cell communication in the frontal lobe (an integrative area) (Fatemi et al., 2008). Moreover, *AQP4* knockout mice have reduced brain swelling in cytotoxic edema, whilst there is a significantly worse result in the case of vasogenic brain edema (Papadopoulos & Verkman, 2007). In the VPA model, it is still not elucidated what type of brain edema is present. Lastly, there are findings linking AQP4 with neuroimmune modulation (Ikeshima-Kataoka, 2016), which represents an important clue in the ASD pathophysiology, since the immune component of this disorder is both relevant and well established (Gottfried et al., 2015).

Noteworthy, as there are few studies on the dynamics of AQP1 and AQP4 in ASD, we think it is important to clarify some points. Despite the common sense that AQP4 is more widely expressed in the brain than AQP1, we observed higher fluorescence levels in AQP1 compared to AQP4 in the control groups in some regions (pSSA and AmR). In astrocytes, the distribution of AQP4 is predominantly in the endfeet projections surrounding vessels; however, its brain concentration varies according to region, with higher levels in the cerebellum and lower expression in the hippocampus, diencephalons, and cortex (Hubbard et al., 2015). Undoubtedly, AQP1

is mainly expressed in the choroid plexus; nevertheless, it is also expressed under normal conditions in other brain structures, such as the brain stem, cerebellum, brain cortex, hippocampus, hypothalamus, and olfactory bulb (Li et al., 2020; Qiu et al., 2014). Beyond that, studies demonstrate neuronal localization of AQP1 in mouse cortical slices, as well as increased cortical levels of AQP1 in Alzheimer's disease models. Moreover, this same work also demonstrates that wild-type animals at 60 days old, present higher amounts of AQP1 protein than AQP4 in cortical homogenates (Park et al., 2021). Finally, in the amygdala region, the human protein atlas demonstrates the mRNA expression of AQP1 (The Human Protein Atlas, n.d.). These studies indicate that the concentration and distribution of AQP 1 and 4 vary according to cell type/domain and brain region, which corroborates our present study regarding the brain region.

The increased GFAP-immunofluorescence and number of GFAP⁺-astrocytes in mPFC and pSSA by prenatal exposure to VPA corroborate with previous studies showing neuroglial activation in both ASD patients and animal models (Bristol Silvestrin et al., 2013; Edmonson et al., 2014; Vargas et al., 2005; Zhao et al., 2019). Here, we observed an important preventive effect of RSV in the mPFC, demonstrated in the decrease of GFAP immunofluorescence. Based on previous data, that indicate the neuroprotective effect of lower doses of RSV in hippocampus slices (emphasizing the important role of RSV in improving glutamate uptake by astrocytes and modulate the synaptic plasticity) (Bobermin et al., 2012; De Almeida et al., 2008; Quincozes-Santos et al., 2013; Quincozes-Santos & Gottfried, 2011), and an improvement in neuroinflammation (an ASD hallmark) in an ASD-animal model (Ahmad et al., 2018; Bhandari & Kuhad, 2017), it would be possible that also in this context, we have a beneficial effect on astrocyte metabolism and function, since this treatment is effective in ameliorates several behavioral impairments in VPA animal model (Bambini-Junior et al., 2014; Fontes-Dutra et al., 2018; Hirsch et al., 2018).

Despite some studies demonstrated no alterations in astrocyte parameters in ASD post mortem tissues (T. T. Lee et al., 2017; Morgan et al., 2014), animal models of fragile X syndrome (a disorder with a high prevalence of ASD) present a specific disruption in the constitution of the deeper layers, besides presenting an increased number of astrocytes (F. Lee et al., 2019). Therefore, alterations in the laminar constitution could influence directly the distribution of astrocytes. The dynamics of cortical disorganization is widely described in ASD. An event like acute

neuroinflammation, with increased levels of brain cytokines, may contribute to synaptic reorganization, which results in long-term alterations regarding hyperexcitability of the whole neural circuitry (Clarkson et al., 2017). One of the most relevant findings in patients with ASD is the identification of disturbance in the organization of the minicolumns (Casanova, 2007) and the presence of patches with loss of layer delimitation in the cortex (DeNardo et al., 2015; Stoner et al., 2014), being the deeper cortical layers the most affected.

In hippocampus and AmR, we observed only effects of RSV treatment. A possible explanation for this effect observed in the amygdala region is that the amygdalar nuclei originate at different times between embryonic day E10-E12 in rats, before the induction of the animal model (in E12.5), and during the prenatal treatment with RSV (between E6.5 to E18.5) (Soma et al., 2009). Although the embryonic origin of the hippocampus starting from E15 (Hayashi et al., 2015), the effects of prenatal exposure to VPA seem to be progressive and of late-onset (Santos-Terra, *unpublished observations*). Despite being a molecule with important neuroprotective effects already described, RSV was able to cause changes in the hippocampus at P30. Considering the progressive effect of VPA in adulthood, maybe RSV develops an earlier cellular background to better support the progressive damage induced by VPA.

One of the major theories regarding ASD pathophysiology refers to the electrophysiological changes, mainly the imbalance between excitation and inhibition. The presence of epilepsy or seizure episodes in approximately 30% of individuals with ASD reinforces the excitatory profile predominant in ASD (Spence & Schneider, 2009). In response to this hyperexcitability and chronic neuroinflammation, might be observed proliferation and hypertrophy of the astrocytes, which acquire a reactive profile (Poskanzer & Molofsky, 2018), due to several roles, including K⁺ buffering. The extracellular K⁺ is critical for defining the resting potential of neurons and astrocyte membranes, and mechanisms for removing this ion from the synaptic cleft are vital to maintaining cerebral homeostasis (Bellot-Saez et al., 2017). One mechanism of K⁺ uptake by glial cells is through the action of internal rectifying channels of K⁺ (Kir) (Olsen et al., 2015). This is particularly important since AQP4 and Kir4.1 are highly overlapping channels in the astrocytic end-feet (Strohschein et al., 2011) and probably AQP4 is required to sustain efficient K⁺ clearance, considering the association of water flux alteration and increasing intensity of epileptic seizures (Amiry-Moghaddam et al., 2003), and a delay in K⁺ buffering in AQP4-null mice (Lu et al., 2008).

Considering all data, we hypothesized that the brain impairments induced by the VPA model include a neuroinflammation background triggered in the developing brain of the embryo, which contributes to the increased BBB permeability (and consequently edema due to the entry of water and inflammatory infiltrate). In consequence, there is a decrease in the levels of AQP1 and AQP4 to maintain water homeostasis in the brain. In parallel, neuroinflammation triggers the excitotoxicity process, leading to a reactive astrocytic phenotype. The increased astrocytic activity leads to an increased need for K⁺ buffering, which in turn increases Kir4.1 and, consequently, AQP4 levels in a region-specific manner (which, in turn, could be the main onset to brain edema formation). The fingerprinting caused by VPA happens in multiple regions; since pSSA is a primary processing area, both the impact caused by VPA and the prevention mechanisms by RSV may be more expressive and less complex than those occurring in mPFC, an associative and more complex region. Here, RSV prevents successfully the impairments regarding BBB permeability and the increase of AQP4 in the pSSA, as well as decreases GFAP antibody labeling in the mPFC, indicating a lower glial reactivity. Thereby, based on several shreds of evidence that point to RSV as a stabilizer of the neural environment, RSV could also normalize K⁺ levels and restructure synaptic connections in pSSA considering the co-localization of AQP4 and Kir4.1 channels.

5. CONCLUDING REMARKS

In summary, we demonstrated that prenatal exposure to VPA alters the bodyweight of the animals, as well as induces brain edema, and increases the permeability of BBB. In addition, there was an altered AQP profile in region-dependent in VPA-exposed animals and GFAP augmented expression. RSV was able to prevent important changes in GFAP⁺ astrocytes and in AQP4 in the pSSA. The neuroprotective role of the RSV in this model shed some light on pathways possibly associated with the alterations induced by VPA along with neuroimmune changes also observed in ASD individuals. Taken together, the present data emphasize the investigation of the mechanisms involved in the neuroimmunological issues as a promising strategy in the understanding of biological pathways in ASD pathophysiology.

REFERENCES

- Abbott, N. J. (2013). Blood-brain barrier structure and function and the challenges for CNS drug delivery. *Journal of Inherited Metabolic Disease*, *36*(3), 437–449. <https://doi.org/10.1007/s10545-013-9608-0>
- Ahmad, S. F., Ansari, M. A., Nadeem, A., Bakheet, S. A., Alzahrani, M. Z., Alshammari, M. A., Alanazi, W. A., Alasmari, A. F., & Attia, S. M. (2018). Resveratrol attenuates pro-inflammatory cytokines and activation of JAK1-STAT3 in BTBR T+ Itpr3tf/J autistic mice. *European Journal of Pharmacology*, *829*, 70–78. <https://doi.org/10.1016/j.ejphar.2018.04.008>
- Akdemir, G., Kaymaz, F., Gursoy-Özdemir, Y., Akalan, N., & Akdemir, E. (2016). The time course changes in expression of aquaporin 4 and aquaporin 1 following global cerebral ischemic edema in rat. *Surgical Neurology International*, *7*(1). <https://doi.org/10.4103/2152-7806.173316>
- Amiry-Moghaddam, M., Williamson, A., Palomba, M., Eid, T., De Lanerolle, N. C., Nagelhus, E. A., Adams, M. E., Froehner, S. C., Agre, P., & Ottersen, O. P. (2003). Delayed K⁺ clearance associated with aquaporin-4 mislocalization: Phenotypic defects in brains of α -synaptrophin-null mice. *Proceedings of the National Academy of Sciences of the United States of America*, *100*(23), 13615–13620. <https://doi.org/10.1073/pnas.2336064100>
- APA, A. P. A.-. (2013). *Diagnostic and Statistical Manual of Mental Disorders, Fifth Edition, DSM-V* (Fifth Edit). Washington, DC.
- Aylward, E. H., Minshew, N. J., Field, K., Sparks, B. F., & Singh, N. (2002). Effects of age on brain volume and head circumference in autism. *Neurology*, *59*(2), 175–83.
- Bambini-Junior, V., Zanatta, G., Della Flora Nunes, G., Mueller de Melo, G., Michels, M., Fontes-Dutra, M., Nogueira Freire, V., Riesgo, R., & Gottfried, C. (2014). Resveratrol prevents social deficits in animal model of autism induced by valproic acid. *Neuroscience Letters*. <https://doi.org/10.1016/j.neulet.2014.09.039>
- Bartholomeusz, H. H., Courchesne, E., & Karns, C. M. (2002). Relationship Between Head Circumference and Brain Volume in Healthy Normal Toddlers, Children, and Adults. *Neuropediatrics*, *33*, 232–238.
- Bellot-Saez, A., Kékesi, O., Morley, J. W., & Buskila, Y. (2017). Astrocytic modulation of neuronal excitability through K⁺ spatial buffering. *Neuroscience &*

Biobehavioral Reviews, 77, 87–97.

<https://doi.org/10.1016/J.NEUBIOREV.2017.03.002>

Benga, O., & Huber, V. J. (2012). Brain water channel proteins in health and disease. *Molecular Aspects of Medicine*.

<https://doi.org/10.1016/j.mam.2012.03.008>

Berman, A. Y., Motechin, R. A., Wiesenfeld, M. Y., Holz, M. K., & Einstein, A. (2017). The therapeutic potential of resveratrol: a review of clinical trials. *NPJ Precision Oncology*, 1–17. <https://doi.org/10.1038/s41698-017-0038-6>.The

Bhandari, R., & Kuhad, A. (2017). Resveratrol suppresses neuroinflammation in the experimental paradigm of autism spectrum disorders. *Neurochemistry International*, 103, 8–23. <https://doi.org/10.1016/j.neuint.2016.12.012>

Bobermin, L. D., Quincozes-Santos, A., Guerra, M. C., Leite, M. C., Souza, D. O., Gonçalves, C. A., & Gottfried, C. (2012). Resveratrol Prevents Ammonia Toxicity in Astroglial Cells. *PLoS ONE*, 7(12), 52164.

<https://doi.org/10.1371/journal.pone.0052164>

Bristot Silvestrin, R., Bambini-Junior, V., Galland, F., Daniele Bobermim, L., Quincozes- Santos, A., Torres Abib, R., Zanotto, C., Batassini, C., Brolese, G., Gonçalves, C. A., Riesgo, R., & Gottfried, C. (2013). Animal model of autism induced by prenatal exposure to valproate: Altered glutamate metabolism in the hippocampus. *Brain Research*. <https://doi.org/10.1016/j.brainres.2012.11.048>

Casanova, M. F. (2007). The Neuropathology of Autism. *Brain Pathology*, 17(4), 422–433. <https://doi.org/10.1111/j.1750-3639.2007.00100.x>

Christensen, J., Grønborg, T. K., Sørensen, M. J., Schendel, D., Parner, E. T., Pedersen, L. H., & Vestergaard, M. (2013). Prenatal Valproate Exposure and Risk of Autism Spectrum Disorders and Childhood Autism. *JAMA*, 1696–1703. <https://doi.org/10.1001/jama.2013.2270>

Clarkson, B. D. S., Kahoud, R. J., McCarthy, C. B., & Howe, C. L. (2017).

Inflammatory cytokine-induced changes in neural network activity measured by waveform analysis of high-content calcium imaging in murine cortical neurons. *Scientific Reports*, 7(1), 9037. <https://doi.org/10.1038/s41598-017-09182-5>

De Almeida, L. M. V., Piñeiro, C. C., Leite, M. C., Brolese, G., Leal, R. B., Gottfried, C., & Gonçalves, C. A. (2008). Protective effects of resveratrol on hydrogen peroxide induced toxicity in primary cortical astrocyte cultures. *Neurochemical Research*, 33(1), 8–15. <https://doi.org/10.1007/s11064-007-9399-5>

- Deckmann, I., Schwingel, G. B., Fontes-Dutra, M., Bambini-Junior, V., & Gottfried, C. (2018). Neuroimmune Alterations in Autism: A Translational Analysis Focusing on the Animal Model of Autism Induced by Prenatal Exposure to Valproic Acid. *Neuroimmunomodulation*, 25(5–6), 285–299. <https://doi.org/10.1159/000492113>
- DeNardo, L. A., Berns, D. S., DeLoach, K., & Luo, L. (2015). Connectivity of mouse somatosensory and prefrontal cortex examined with trans-synaptic tracing. *Nature Neuroscience*, 18(11), 1687–1697. <https://doi.org/10.1038/nn.4131>
- Edmonson, C., Ziats, M. N., & Rennert, O. M. (2014). *Altered glial marker expression in autistic post-mortem prefrontal cortex and cerebellum*. <https://doi.org/10.1186/2040-2392-5-3>
- Emerson, R. W., Adams, C., Nishino, T., Hazlett, H. C., Wolff, J. J., Zwaigenbaum, L., Constantino, J. N., Shen, M. D., Swanson, M. R., Elison, J. T., Kandala, S., Estes, A. M., Botteron, K. N., Collins, L., Dager, S. R., Evans, A. C., Gerig, G., Gu, H., Mckinstry, R. C., Paterson, S., Schultz, R. T., Styner, M., Schlaggar, B. L., Pruett, J. R., & Piven, J. (2017). Functional neuroimaging of high-risk 6-month-old infants predicts a diagnosis of autism at 24 months of age. *Science Translational Medicine*, 9(393). <https://doi.org/10.1126/scitranslmed.aag2882>
- Estes, M. L., & McAllister, A. K. (2016). Maternal immune activation: Implications for neuropsychiatric disorders. *Science*, 353(6301), 772–777. <https://doi.org/10.1126/science.aag3194>
- Fatemi, S. H., Folsom, T. D., Reutiman, T. J., & Lee, S. (2008). Expression of astrocytic markers aquaporin 4 and connexin 43 is altered in brains of subjects with autism. *Synapse*. <https://doi.org/10.1002/syn.20519>
- Fontes-Dutra, M., Santos-Terra, J., Deckmann, I., Brum Schwingel, G., Della-Flora Nunes, G., Hirsch, M. M., Bauer-Negrini, G., Riesgo, R. S., Bambini-Júnior, V., Hedin-Pereira, C., & Gottfried, C. (2018). Resveratrol Prevents Cellular and Behavioral Sensory Alterations in the Animal Model of Autism Induced by Valproic Acid. *Frontiers in Synaptic Neuroscience*, 10, 9. <https://doi.org/10.3389/fnsyn.2018.00009>
- Frémont, L. (2000). Biological effects of resveratrol. *Life Sciences*, 66(8), 663–673. [https://doi.org/10.1016/S0024-3205\(99\)00410-5](https://doi.org/10.1016/S0024-3205(99)00410-5)
- Gottfried, C., Bambini-Junior, V., Francis, F., Riesgo, R., & Savino, W. (2015). The Impact of Neuroimmune Alterations in Autism Spectrum Disorder. *Frontiers in Psychiatry*, 6, 121. <https://doi.org/10.3389/fpsy.2015.00121>

- Hayashi, K., Kubo, K. I., Kitazawa, A., & Nakajima, K. (2015). Cellular dynamics of neuronal migration in the hippocampus. *Frontiers in Neuroscience*, 9(APR), 135. <https://doi.org/10.3389/fnins.2015.00135>
- Hazlett, H. C., Poe, M., Gerig, G., Styner, M., Chappell, C., Smith, R. G., Vachet, C., & Piven, J. (2011). Early Brain Overgrowth in Autism Associated with an Increase in Cortical Surface Area Before Age 2 years. *Archives of General Psychiatry*, 68(5), 467–476. <https://doi.org/10.1001/archgenpsychiatry.2011.39.Early>
- Hirsch, M. M., Deckmann, I., Fontes-Dutra, M., Bauer-Negrini, G., Della-Flora Nunes, G., Nunes, W., Rabelo, B., Riesgo, R., Margis, R., Bambini-Junior, V., & Gottfried, C. (2018). Behavioral alterations in autism model induced by valproic acid and translational analysis of circulating microRNA. *Food and Chemical Toxicology*, 115(February), 336–343. <https://doi.org/10.1016/j.fct.2018.02.061>
- Hubbard, J. A., Hsu, M. S., Seldin, M. M., & Binder, D. K. (2015). Expression of the astrocyte water channel aquaporin-4 in the mouse brain. *ASN Neuro*, 7(5). <https://doi.org/10.1177/1759091415605486>
- Ikeshima-Kataoka, H. (2016). Neuroimmunological Implications of AQP4 in Astrocytes. *International Journal of Molecular Sciences*, 17(8), 1306. <https://doi.org/10.3390/ijms17081306>
- Kalra, S., Burbelo, P. D., Bayat, A., Ching, K. H., Thurm, A., Iadarola, M. J., & Swedo, S. E. (2015). No evidence of antibodies against GAD65 and other specific antigens in children with autism. *BBACLI*, 4, 81–84. <https://doi.org/10.1016/j.bbacli.2015.08.001>
- Koushki, M., Lakzaei, M., Khodabandehloo, H., Hosseini, H., Meshkani, R., & Panahi, G. (2020). Therapeutic effect of resveratrol supplementation on oxidative stress: A systematic review and meta-analysis of randomised controlled trials. *Postgraduate Medical Journal*, 96(1134), 197–205. <https://doi.org/10.1136/postgradmedj-2019-136415>
- Kumar, H., & Sharma, B. (2016a). Memantine ameliorates autistic behavior, biochemistry & blood brain barrier impairments in rats. *Brain Research Bulletin*, 124, 27–39. <https://doi.org/10.1016/j.brainresbull.2016.03.013>
- Kumar, H., & Sharma, B. (2016b). Minocycline ameliorates prenatal valproic acid induced autistic behaviour, biochemistry and blood brain barrier impairments in rats. *Brain Research*. <https://doi.org/10.1016/j.brainres.2015.10.052>

- Kumar, H., Sharma, B. M., & Sharma, B. (2015). Benefits of agomelatine in behavioral, neurochemical and blood brain barrier alterations in prenatal valproic acid induced autism spectrum disorder. *Neurochemistry International*.
<https://doi.org/10.1016/j.neuint.2015.10.007>
- Le Belle, J. E., Sperry, J., Ngo, A., Ghochani, Y., Laks, D. R., López-Aranda, M., Silva, A. J., & Kornblum, H. I. (2014). Maternal inflammation contributes to brain overgrowth and autism-associated behaviors through altered redox signaling in stem and progenitor cells. *Stem Cell Reports*, 3(5), 725–34.
<https://doi.org/10.1016/j.stemcr.2014.09.004>
- Lee, F., Lai, T., Su, P., & Liu, F. (2019). Altered cortical Cytoarchitecture in the Fmr1 knockout mouse. *Molecular Brain*, 12(1), 56. <https://doi.org/10.1186/s13041-019-0478-8>
- Lee, J.-A., Ha, S. K., Cho, E., & Choi, I. (2015). Resveratrol as a Bioenhancer to Improve Anti-Inflammatory Activities of Apigenin. *Nutrients*, 7(11), 9650–61.
<https://doi.org/10.3390/nu7115485>
- Lee, T. T., Skafidas, E., Dottori, M., Zantomio, D., Pantelis, C., Everall, I., & Chana, G. (2017). No preliminary evidence of differences in astrocyte density within the white matter of the dorsolateral prefrontal cortex in autism. *Molecular Autism*, 8(1), 64. <https://doi.org/10.1186/s13229-017-0181-5>
- Li, Q., Aalling, N. N., Förstera, B., Ertürk, A., Nedergaard, M., Møllgård, K., & Xavier, A. L. R. (2020). Aquaporin 1 and the Na⁺/K⁺/2Cl⁻ cotransporter 1 are present in the leptomeningeal vasculature of the adult rodent central nervous system. *Fluids and Barriers of the CNS*, 17(1), 15. <https://doi.org/10.1186/s12987-020-0176-z>
- Lowry, O., Rosebrough, N., Farr, A., & Randall, R. (1951). Protein measurement with the Folin phenol reagent. *The Journal of Biological Chemistry*, 193(1), 265–75.
- Lu, D. C., Zhang, H., Zador, Z., & Verkman, A. S. (2008). Impaired olfaction in mice lacking aquaporin-4 water channels. *The FASEB Journal*, 22(9), 3216–3223.
<https://doi.org/10.1096/fj.07-104836>
- Maenner, M. J., Shaw, K. A., Baio, J., Washington, A., Patrick, M., DiRienzo, M., Christensen, D. L., Wiggins, L. D., Pettygrove, S., Andrews, J. G., Lopez, M., Hudson, A., Baroud, T., Schwenk, Y., White, T., Rosenberg, C. R., Lee, L.-C., Harrington, R. A., Huston, M., Hewitt, A., Esler, A., Hall-Lande, J., Poynter, J. N., Hallas-Muchow, L., Constantino, J. N., Fitzgerald, R. T., Zahorodny, W.,

- Shenouda, J., Daniels, J. L., Warren, Z., Vehorn, A., Salinas, A., Durkin, M. S., & Dietz, P. M. (2020). Prevalence of Autism Spectrum Disorder Among Children Aged 8 Years — Autism and Developmental Disabilities Monitoring Network, 11 Sites, United States, 2016. *MMWR. Surveillance Summaries*, *69*(4), 1–12.
<https://doi.org/10.15585/mmwr.ss6904a1>
- Mohammadshahi, M., Haidari, F., & Soufi, F. G. (2014). Chronic resveratrol administration improves diabetic cardiomyopathy in part by reducing oxidative stress. *Cardiology Journal*, *21*(1), 39–46. <https://doi.org/10.5603/CJ.a2013.0051>
- Mony, T. J., Lee, J. W., Dreyfus, C., DiCicco-Bloom, E., & Lee, H. J. (2016). Valproic Acid Exposure during Early Postnatal Gliogenesis Leads to Autistic-like Behaviors in Rats. *Clinical Psychopharmacology and Neuroscience: The Official Scientific Journal of the Korean College of Neuropsychopharmacology*, *14*(4), 338–344. <https://doi.org/10.9758/cpn.2016.14.4.338>
- Morgan, J. T., Barger, N., Amaral, D. G., & Schumann, C. M. (2014). Stereological study of amygdala glial populations in adolescents and adults with autism spectrum disorder. *PLoS ONE*, *9*(10), 110356.
<https://doi.org/10.1371/journal.pone.0110356>
- Moussa, C., Hebron, M., Huang, X., Ahn, J., Rissman, R. A., Aisen, P. S., & Turner, R. S. (2017). Resveratrol regulates neuro-inflammation and induces adaptive immunity in Alzheimer's disease. *Journal of Neuroinflammation*, *14*(1).
<https://doi.org/10.1186/s12974-016-0779-0>
- Nagelhus, E. A., & Ottersen, O. P. (2013). Physiological Roles of Aquaporin-4 in Brain. *Physiological Reviews*, *93*(4), 1543–1562.
<https://doi.org/10.1152/physrev.00011.2013>
- Olsen, M. L., Khakh, B. S., Skatchkov, S. N., Zhou, M., Lee, C. J., & Rouach, N. (2015). New Insights on Astrocyte Ion Channels: Critical for Homeostasis and Neuron-Glia Signaling. *The Journal of Neuroscience: The Official Journal of the Society for Neuroscience*, *35*(41), 13827–35.
<https://doi.org/10.1523/JNEUROSCI.2603-15.2015>
- Oshio, K., Song, Y., Verkman, A. S., & Manley, G. T. (2003). Aquaporin-1 deletion reduces osmotic water permeability and cerebrospinal fluid production. *Acta Neurochirurgica. Supplement*, *86*, 525–8. Retrieved from <http://www.ncbi.nlm.nih.gov/pubmed/14753499>
- Papadopoulos, M. C., & Verkman, A. S. (2007). Aquaporin-4 and brain edema.

Pediatric Nephrology. <https://doi.org/10.1007/s00467-006-0411-0>

- Park, J., Madan, M., Chigurupati, S., Baek, S. H., Cho, Y., Mughal, M. R., Yu, A., Chan, S. L., Pattisapu, J. V., Mattson, M. P., & Jo, D. G. (2021). Neuronal aquaporin 1 inhibits amyloidogenesis by suppressing the interaction between beta-secretase and amyloid precursor protein. *Journals of Gerontology - Series A Biological Sciences and Medical Sciences*, *76*(1), 23–31. <https://doi.org/10.1093/GERONA/GLAA068>
- Petrelli, F., Pucci, L., & Bezzi, P. (2016). Astrocytes and Microglia and Their Potential Link with Autism Spectrum Disorders. *Frontiers in Cellular Neuroscience*, *10*, 21. <https://doi.org/10.3389/fncel.2016.00021>
- Poskanzer, K. E., & Molofsky, A. V. (2018). Dynamism of an Astrocyte In Vivo: Perspectives on Identity and Function. *Annual Review of Physiology*, *80*, 143–157. <https://doi.org/10.1146/annurev-physiol-021317-121125>
- Qiu, B., Li, X., Sun, X., Wang, Y., Jing, Z., Zhang, X., & Wang, Y. (2014). Overexpression of aquaporin-1 aggravates hippocampal damage in mouse traumatic brain injury models. *Molecular Medicine Reports*, *9*(3), 916–922. <https://doi.org/10.3892/mmr.2014.1899>
- Quincozes-Santos, A., Bobermin, L. D., Latini, A., Wajner, M., Souza, D. O., Gonçalves, C. A., & Gottfried, C. (2013). Resveratrol Protects C6 Astrocyte Cell Line against Hydrogen Peroxide-Induced Oxidative Stress through Heme Oxygenase 1. *PLoS ONE*, *8*(5), 64372. <https://doi.org/10.1371/journal.pone.0064372>
- Quincozes-Santos, A., & Gottfried, C. (2011). Resveratrol modulates astroglial functions: Neuroprotective hypothesis. *Annals of the New York Academy of Sciences*, *1215*(1), 72–78. <https://doi.org/10.1111/j.1749-6632.2010.05857.x>
- Rahman, I., Marwick, J., & Kirkham, P. (2004). Redox modulation of chromatin remodeling: Impact on histone acetylation and deacetylation, NF- κ B and pro-inflammatory gene expression. *Biochemical Pharmacology*, *68*(6), 1255–1267. <https://doi.org/10.1016/j.bcp.2004.05.042>
- Reinhard, S. M., Razak, K., & Ethell, I. M. (2015). A delicate balance: role of MMP-9 in brain development and pathophysiology of neurodevelopmental disorders. *Frontiers in Cellular Neuroscience*, *9*, 280. <https://doi.org/10.3389/fncel.2015.00280>
- Rosu, G. C., Pirici, I., Grigorie, A. A., Istrate-Ofiteru, A. M., Iovan, L., Tudorica, V., &

- Pirici, D. (2019). Distribution of Aquaporins 1 and 4 in the Central Nervous System. *Current Health Sciences Journal*, 45(2), 218–226.
<https://doi.org/10.12865/CHSJ.45.02.14>
- Roudnicky, F., Kim, B. K., Lan, Y., Schmucki, R., Küppers, V., Christensen, K., Graf, M., Patsch, C., Burcin, M., Meyer, C. A., Westenskow, P. D., & Cowan, C. A. (2020). Identification of a combination of transcription factors that synergistically increases endothelial cell barrier resistance. *Scientific Reports*, 10(1), 1–9.
<https://doi.org/10.1038/s41598-020-60688-x>
- Roulet, F. I., Lai, J. K. Y., & Foster, J. A. (2013). In utero exposure to valproic acid and autism - A current review of clinical and animal studies. *Neurotoxicology and Teratology*, 36, 47–56. <https://doi.org/10.1016/j.ntt.2013.01.004>
- Sacco, R., Gabriele, S., & Persico, A. M. (2015). Head circumference and brain size in autism spectrum disorder: A systematic review and meta-analysis. *Psychiatry Research - Neuroimaging*, 234(2), 239–251.
<https://doi.org/10.1016/j.psychres.2015.08.016>
- Sánchez-Fidalgo, S., Cárdeno, A., Villegas, I., Talero, E., & de la Lastra, C. A. (2010). Dietary supplementation of resveratrol attenuates chronic colonic inflammation in mice. *European Journal of Pharmacology*, 633(1–3), 78–84.
<https://doi.org/10.1016/J.EJPHAR.2010.01.025>
- Sawda, C., Moussa, C., & Turner, R. S. (2017). Resveratrol for alzheimer's disease. *Annals of the New York Academy of Sciences*, 1403(1), 142–149.
<https://doi.org/10.1111/nyas.13431>
- Schneider, T., & Przewłocki, R. (2005). Behavioral Alterations in Rats Prenatally Exposed to Valproic Acid: Animal Model of Autism. *Neuropsychopharmacology*, 30(1), 80–89. <https://doi.org/10.1038/sj.npp.1300518>
- Simões, L. R., Sangiogo, G., Tashiro, M. H., Generoso, J. S., Faller, C. J., Domingui, D., Mastella, G. A., Scaini, G., Giridharan, V. V., Michels, M., Florentino, D., Petronilho, F., Réus, G. Z., Dal-Pizzol, F., Zugno, A. I., & Barichello, T. (2018). Maternal immune activation induced by lipopolysaccharide triggers immune response in pregnant mother and fetus, and induces behavioral impairment in adult rats. *Journal of Psychiatric Research*, 100, 71–83.
<https://doi.org/10.1016/j.jpsychires.2018.02.007>
- Smith, V., & Brown, N. (2014). Prenatal valproate exposure and risk of autism spectrum disorders and childhood autism. *Archives of Disease in Childhood*.

- Education and Practice Edition*, 99(5), 198. <https://doi.org/10.1136/archdischild-2013-305636>
- Soma, M., Aizawa, H., Ito, Y., Maekawa, M., Osumi, N., Nakahira, E., Okamoto, H., Tanaka, K., & Yuasa, S. (2009). Development of the mouse amygdala as revealed by enhanced green fluorescent protein gene transfer by means of in utero electroporation. *The Journal of Comparative Neurology*, 513(1), 113–128. <https://doi.org/10.1002/cne.21945>
- Spence, S. J., & Schneider, M. T. (2009). The role of epilepsy and epileptiform EEGs in autism spectrum disorders. *Pediatric Research*, 65(6), 599–606. <https://doi.org/10.1203/PDR.0b013e31819e7168>
- Ssucharewa, G. E. (1926). Die schizoiden Psychopathien im Kindesalter. (Part 1 of 2). *European Neurology*, 60(3–4), 235–247. <https://doi.org/10.1159/000190478>
- Stamatovic, S. M., Dimitrijevic, O. B., Keep, R. F., & Andjelkovic, A. V. (2006). Inflammation and brain edema: new insights into the role of chemokines and their receptors. In *Brain Edema XIII* (Vol. 96, pp. 444–450). Vienna: Springer-Verlag. https://doi.org/10.1007/3-211-30714-1_91
- Stoner, R., Chow, M. L., Boyle, M. P., Sunkin, S. M., Mouton, P. R., Roy, S., Wynshaw-Boris, A., Colamarino, S. A., Lein, E. S., & Courchesne, E. (2014). Patches of disorganization in the neocortex of children with autism. *The New England Journal of Medicine*, 370(13), 1209–1219. <https://doi.org/10.1056/NEJMoa1307491>
- Strohschein, S., Hüttmann, K., Gabriel, S., Binder, D. K., Heinemann, U., & Steinhäuser, C. (2011). Impact of aquaporin-4 channels on K⁺ buffering and gap junction coupling in the hippocampus. *GLIA*, 59(6), 973–980. <https://doi.org/10.1002/glia.21169>
- Tambur, A. R., & Roitberg, B. (2005). Immunology of the central nervous system. *Neurological Research*, 27(7), 675–678. <https://doi.org/10.1179/016164105X49544>
- Tang, B. L. (2010). Resveratrol is neuroprotective because it is not a direct activator of Sirt1—A hypothesis. *Brain Research Bulletin*, 81(4–5), 359–361. <https://doi.org/10.1016/J.BRAINRESBULL.2009.12.007>
- The Human Protein Atlas. (n.d.). Tissue expression of AQP1 - Staining in Amygdala - The Human Protein Atlas. Retrieved June 7, 2021, from <https://www.proteinatlas.org/ENSG00000240583-AQP1/tissue/Amygdala>

- Vang, O., Ahmad, N., Baile, C. A., Baur, J. A., Brown, K., Csiszar, A., Das, D. K., Delmas, D., Gottfried, C., Lin, H.-Y., Ma, Q.-Y., Mukhopadhyay, P., Nalini, N., Pezzuto, J. M., Richard, T., Shukla, Y., Surh, Y.-J., Szekeres, T., Szkudelski, T., Walle, T., & Wu, J. M. (2011). What Is New for an Old Molecule? Systematic Review and Recommendations on the Use of Resveratrol. *PLoS ONE*, *6*(6), e19881. <https://doi.org/10.1371/journal.pone.0019881>
- Vargas, D. L., Nascimbene, C., Krishnan, C., Zimmerman, A. W., & Pardo, C. A. (2005). Neuroglial activation and neuroinflammation in the brain of patients with autism. *Ann Neurol*, *57*(1), 67–81. <https://doi.org/10.1002/ana.20315>
- Voineagu, I., Wang, X., Johnston, P., Lowe, J. K., Tian, Y., Horvath, S., Mill, J., Cantor, R. M., Blencowe, B. J., & Geschwind, D. H. (2011). Transcriptomic analysis of autistic brain reveals convergent molecular pathology. *Nature*, *474*(7351), 380–384. <https://doi.org/10.1038/nature10110>
- Wei, H., Wang, S., Zhen, L., Yang, Q., Wu, Z., Lei, X., Lv, J., Xiong, L., & Xue, R. (2015). Resveratrol Attenuates the Blood-Brain Barrier Dysfunction by Regulation of the MMP-9/TIMP-1 Balance after Cerebral Ischemia Reperfusion in Rats. *Journal of Molecular Neuroscience*, *55*(4), 872–879. <https://doi.org/10.1007/s12031-014-0441-1>
- Xiao, M., & Hu, G. (2014). Involvement of Aquaporin 4 in Astrocyte Function and Neuropsychiatric Disorders. *CNS Neuroscience and Therapeutics*. <https://doi.org/10.1111/cns.12267>
- Zamberletti, E., Gabaglio, M., Woolley-Roberts, M., Bingham, S., Rubino, T., & Parolaro, D. (2019). Cannabidiol Treatment Ameliorates Autism-Like Behaviors and Restores Hippocampal Endocannabinoid System and Glia Alterations Induced by Prenatal Valproic Acid Exposure in Rats. *Frontiers in Cellular Neuroscience*, *13*. <https://doi.org/10.3389/fncel.2019.00367>
- Zeidán-Chuliá, F., Salmina, A. B., Malinovskaya, N. A., Noda, M., Verkhatsky, A., & Moreira, J. C. F. (2014). The glial perspective of autism spectrum disorders. *Neuroscience & Biobehavioral Reviews*, *38*, 160–172. <https://doi.org/10.1016/J.NEUBIOREV.2013.11.008>
- Zeldovich, L. (2018). How History Forgot the Woman Who Defined Autism - Scientific American.
- Zhao, H., Wang, Q., Yan, T., Zhang, Y., Xu, H. Juan, Yu, H. peng, Tu, Z., Guo, X., Jiang, Y. hui, Li, X. jiang, Zhou, H., & Zhang, Y. Q. (2019). Maternal valproic

acid exposure leads to neurogenesis defects and autism-like behaviors in non-human primates. *Translational Psychiatry*, 9(1), 1–13.
<https://doi.org/10.1038/s41398-019-0608-1>

Accepted Article

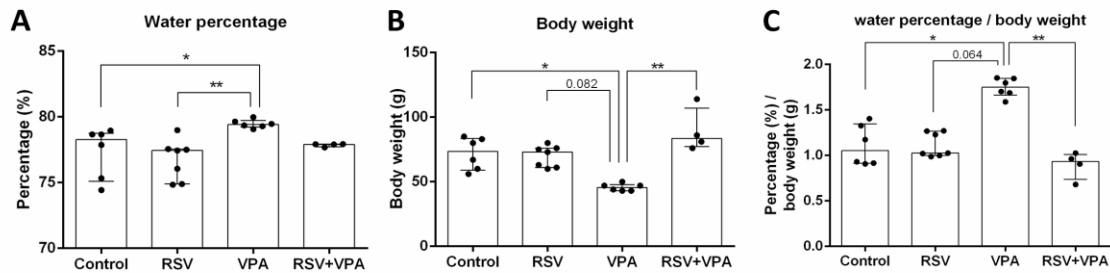


Figure 1 – Brain water content in an animal model of autism and the resveratrol effect (RSV). A) Percentage of water in the whole brain through the difference in wet weight and dry weight. B) Body weight, showing that the animals in the VPA group have lower weight throughout development. C) Proportion of brain fluid volume corrected by the difference in body weight of the animals. Values are shown in median±IQR. Statistical analyses: Kruskal-Wallis. N_{CON} : 5, N_{RSV} : 6, N_{VPA} : 6, $N_{RSV+VPA}$: 4. * $p < 0.05$; ** $p < 0.001$.

Accepted A

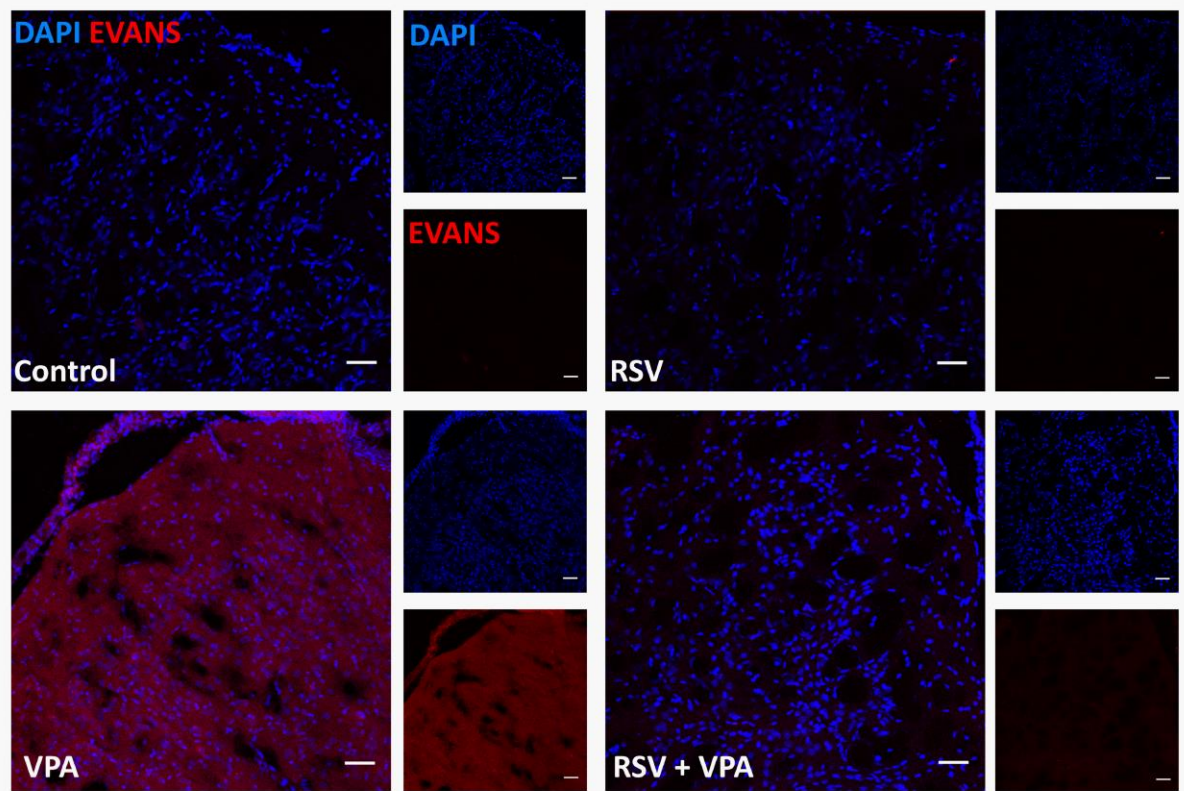


Figure 2 – Permeability of the blood-brain barrier to Evans blue dye. A) Representative images of the anterior cingulate cortex (II/III layers). The nuclear dye DAPI is stained in blue and the fluorescence of Evans blue in red. Scale bar: 50 μm . Statistical analyses: Kruskal-Wallis. N_{CON} : 5, N_{RSV} : 7, N_{VPA} : 4, $N_{\text{RSV+VPA}}$: 4.

Accepted

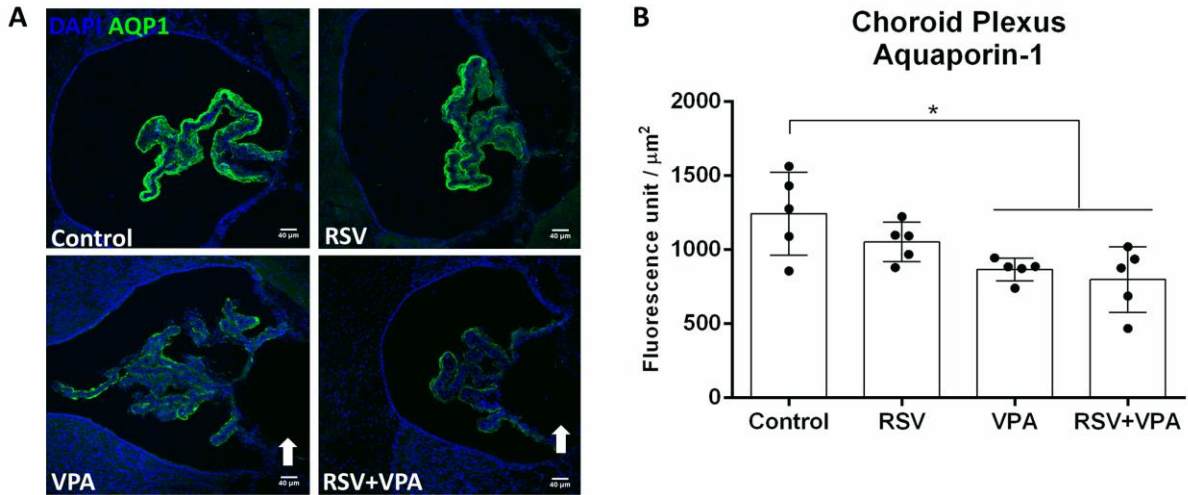


Figure 3 – Distribution of aquaporin 1 (AQP1) in the choroid plexus. (A) Representative images of the immunofluorescent label and (B) graphic representation of the expression of AQP1 in the choroid plexus. Scale bar: 40 μm . Values are shown as mean of fluorescence \pm standard deviation. Statistical analysis: two-way ANOVA followed by Sidak. N = 5. * $p < 0.05$. AQP1 is marked in green and nuclear DAPI dye in blue.

Accepted

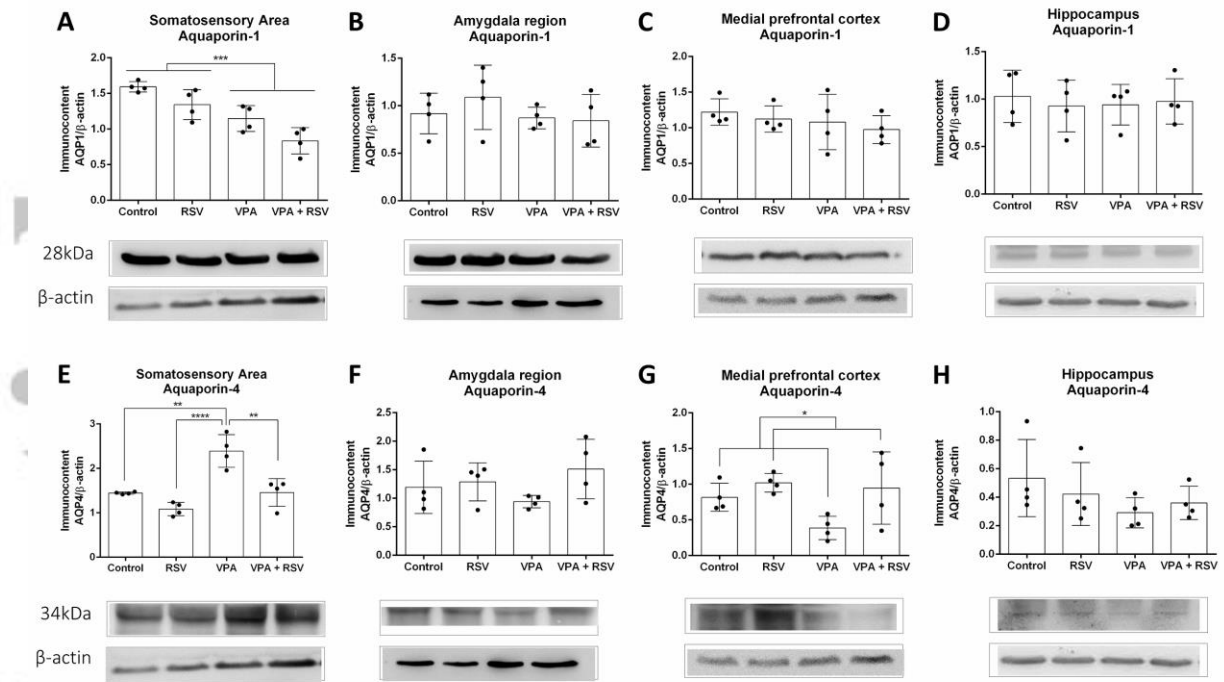


Figure 4 - Immunostaining of aquaporin 1 (AQP1) and AQP4 in different regions of the Central Nervous System. Quantification of AQP1 and AQP4 immunostaining (A)(E) in the primary somatosensory area, (B)(F) in the amygdala region, (C)(G) in the medial prefrontal cortex and (D)(H) in the hippocampus, respectively. The immunostaining of both AQP1 and AQP4 was normalized by the β -actin loading control. Values are shown as mean \pm standard deviation. Statistical analysis: two-way ANOVA followed by Sidak. N = 4. * $p < 0.05$.

Accepted

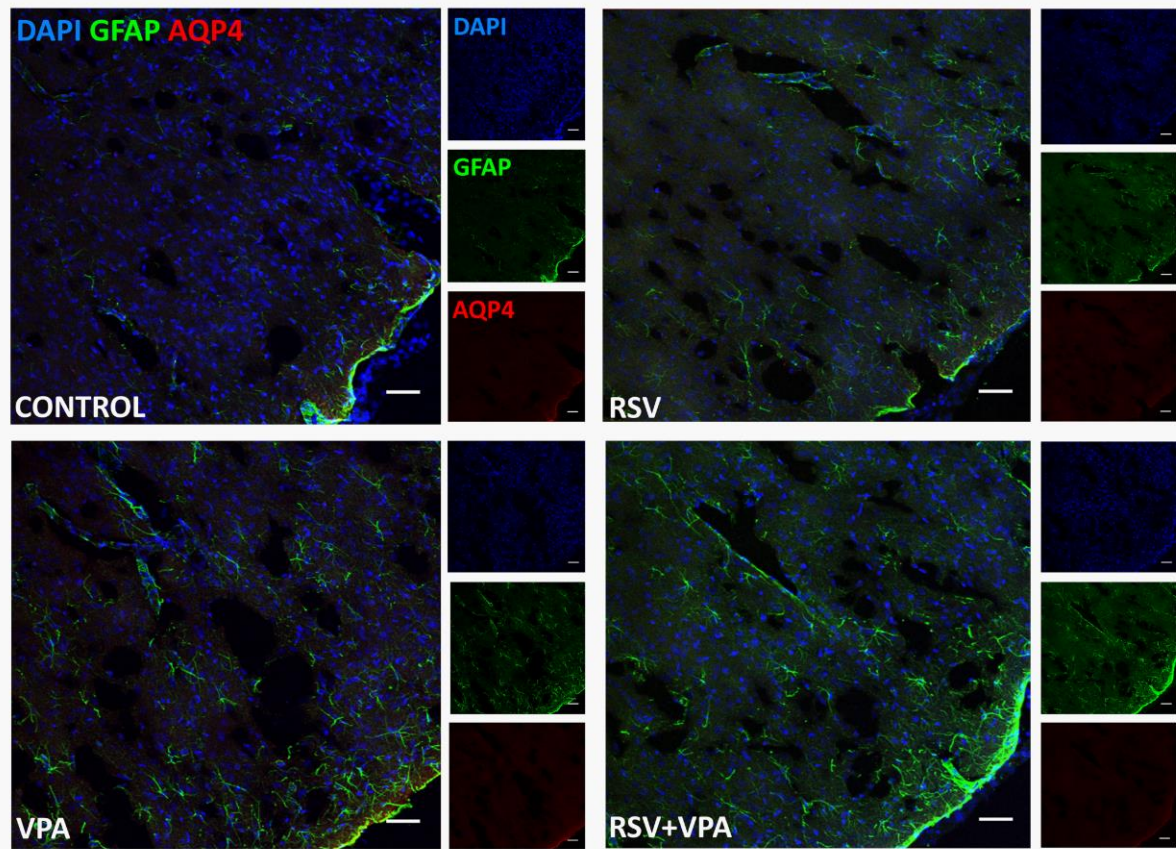


Figure 5 - Analysis of astrocytes in the primary somatosensory area. Representative images of the immunofluorescent labeling of DAPI, GFAP and AQP4 in the primary somatosensory area (II/III) in the different experimental groups. Statistical analysis: two-way ANOVA followed by Sidak. N_{CON} : 5, N_{RSV} : 6, N_{VPA} : 6, $N_{RSV+VPA}$: 5. GFAP is marked in green, AQP4 in red and DAPI nuclear dye in blue. Scale bar: 50 μ m.

Accepted Article

Table 1 – Descriptive statistics of body weight and in proportional brain water content

	Median (IQR)	Chi-Square, df	p Value	Mean rank	Pairwise comparisons
%	CON: 78.27 (75.10±78.74)	14.019, 3	0.003**	CON: 10.00	CON vs RSV: >0.999
	RSV: 77.44 (74.89±77.56)			RSV: 6.86	CON vs VPA: 0.044*
	VPA: 79.41 (79.23±79.73)			VPA: 20.50	CON vs RSV+VPA: >0.999
	RSV+VPA: 77.91 (77.74±77.93)			RSV+VPA: 11.25	RSV vs VPA: 0.002**
					RSV vs RSV+VPA: >0.999
g	CON: 73.50 (59.00±83.50)	15.659, 3	0.001**	CON: 9.50	VPA vs RSV+VPA: 0.208
	RSV: 73.00 (61.00±76.00)			RSV: 10.86	CON vs RSV: >0.999
	VPA: 45.50 (43.00±47.75)			VPA: 20.50	CON vs VPA: 0.030*
	RSV+VPA: 83.50 (77.25±107.00)			RSV+VPA: 5.00	CON vs RSV+VPA: >0.999
					RSV vs VPA: 0.064#
%/g	CON: 1.052 (0.914±1.347)	14.699, 3	0.002**	CON: 14.33	RSV vs RSV+VPA: >0.999
	RSV: 1.025 (0.998±1.268)			RSV: 12.79	CON vs VPA: 0.034*
	VPA: 1.749 (1.663±1.847)			VPA: 3.50	CON vs RSV+VPA: >0.999
	RSV+VPA: 0.934 (0.737±1.009)			RSV+VPA: 19.88	RSV vs VPA: 0.082#
					RSV vs RSV+VPA: 0,570
		VPA vs RSV+VPA: 0.001**			

%: brain water content percentage; **g:** body weight; **%/g:** proportion of brain fluid. p <0.05 was considered significant. *p<0.05, **p<0.01. Statistical analyses: Kruskal-Wallis. N_{CON}: 5, N_{RSV}: 6, N_{VPA}: 6, N_{RSV+VPA}: 4.

Table 2 – Descriptive statistics of Evans blue dye

	Median (IQR)	Chi-Square, df	p Value	Mean rank	Pairwise comparisons
CP	CON: 98.08 (75.07±103.4)	11.674, 3	0.009**	CON: 12.60	CON vs RSV: >0.999
	RSV: 77.09 (56.18±91.46)			RSV: 7.64	CON vs VPA: 0.584
	VPA: 253.6 (150.4±393.0)			VPA: 19.50	CON vs RSV+VPA: >0.999
	RSV+VPA: 72.00 (62.16±88.70)			RSV+VPA: 7.30	RSV vs VPA: 0.014*
					RSV vs RSV+VPA: >0.999
				VPA vs RSV+VPA: 0.020*	
HIP	CON: 100.6 (81.16±122.5)	5.572, 3	0.134	CON: 14.90	CON vs RSV: >0.999
	RSV: 83.16 (63.64±97.31)			RSV: 10.36	CON vs VPA: >0.999
	VPA: 107.4 (57.4±180.5)			VPA: 13.25	CON vs RSV+VPA: 0.149
	RSV+VPA: 68.5 (55.03±75.59)			RSV+VPA: 6.20	RSV vs VPA: >0.999
					RSV vs RSV+VPA: >0.999
				VPA vs RSV+VPA: 0.542	
AmR	CON: 97.14 (90.83±115.4)	7.812, 3	0.050	CON: 15.60	CON vs RSV: 0.381
	RSV: 79.56 (66.98±94.11)			RSV: 8.86	CON vs VPA: >0.999
	VPA: 108.7 (46.77±159.2)			VPA: 14.75	CON vs RSV+VPA: 0.114
	RSV+VPA: 66.17 (44.93±83.03)			RSV+VPA: 6.40	RSV vs VPA: 0.778
					RSV vs RSV+VPA: >0.999
				VPA vs RSV+VPA: 0.269	
pSSA (II/III)	CON: 123.00 (113.7±146.1)	13.541, 3	0.004**	CON: 13.8	CON vs RSV: 0.321
	RSV: 88.71 (78.22±106.4)			RSV: 6.79	CON vs VPA: >0.999
	VPA: 838.6 (624.3±1019.0)			VPA: 19.50	CON vs RSV+VPA: 0.585
	RSV+VPA: 86.19 (78.83±112.4)			RSV+VPA: 7.30	RSV vs VPA: 0.006**
					RSV vs RSV+VPA: >0.999
				VPA vs RSV+VPA: 0.020*	
pSSA (IV/V)	CON: 124.6 (115.4±142.0)	12.855, 3	0.005**	CON: 13.40	CON vs RSV: 0.468
	RSV: 105.9 (62.22±118.5)			RSV: 7.00	CON vs VPA: 0.856
	VPA: 483.9 (321.5±578.7)			VPA: 19.50	CON vs RSV+VPA: 0.757
	RSV+VPA: 95.09 (91.75±120.7)			RSV+VPA: 7.40	RSV vs VPA: 0.008**
					RSV vs RSV+VPA: >0.999
				VPA vs RSV+VPA: 0.022*	
aCC (II/III)	CON: 100.9 (78.63±112.2)	11.670, 3	0.001**	CON: 11.50	CON vs RSV: >0.999
	RSV: 77.78 (74.32±90.65)			RSV: 8.21	CON vs VPA: 0.465
	VPA: 370.1 (279.2±416.7)			VPA: 18.50	CON vs RSV+VPA: 0.690
	RSV+VPA: 71.57 (68.05±95.45)			RSV+VPA: 5.25	RSV vs VPA: 0.033*
					RSV vs RSV+VPA: >0.999
				VPA vs RSV+VPA: 0.009**	
aCC (IV/V)	CON: 86.73 (81.27±99.31)	10.801, 3	0.013*	CON: 11.20	CON vs RSV: >0.999
	RSV: 78.16 (77.02±107.5)			RSV: 6.86	CON vs VPA: 0.391
	VPA: 423.9 (335.2±447.6)			VPA: 18.50	CON vs RSV+VPA: >0.999
	RSV+VPA: 80.25 (78.98±92.59)			RSV+VPA: 8.00	RSV vs VPA: 0.010*
					RSV vs RSV+VPA: >0.999
				VPA vs RSV+VPA: 0.071#	
PrL (II/III)	CON: 78.56 (71.57±100.8)	9.926, 3	0.019*	CON: 8.40	CON vs RSV: >0.999
	RSV: 79.78 (74.39±106.5)			RSV: 9.71	CON vs VPA: 0.065#
	VPA: 378.2 (230.0±422.7)			VPA: 18.50	CON vs RSV+VPA: >0.999
	RSV+VPA: 73.94 (64.44±89.42)			RSV+VPA: 6.50	RSV vs VPA: 0.106
					RSV vs RSV+VPA: >0.999
				VPA vs RSV+VPA: 0.024*	
PrL (IV/V)	CON: 82.80 (78.15±99.0)	9.653, 3	0.022*	CON: 9.70	CON vs RSV: >0.999
	RSV: 86.23 (71.51±108.7)			RSV: 9.71	CON vs VPA: 0.219
	VPA: 364.9 (172.0±378.0)			VPA: 18.00	CON vs RSV+VPA: >0.999
	RSV+VPA: 69.02 (63.39±89.87)			RSV+VPA: 5.38	RSV vs VPA: 0.152
					RSV vs RSV+VPA: >0.999
				VPA vs RSV+VPA: 0.015*	

IL (II/III)	CON: 81.6 (80.25±93.42)	9.060, 3	0.028*	CON: 9.40	CON vs RSV: >0.999
	RSV: 79.34 (71.30±104.2)			RSV: 7.93	CON vs VPA: 0.141
	VPA: 232.9 (141.5±351.4)			VPA: 18.38	CON vs RSV+VPA: >0.999
	RSV+VPA: 78.77 (68.97±106.5)			RSV+VPA: 8.50	RSV vs VPA: 0.029*
					VPA vs RSV+VPA: 0.109
IL (IV/V)	CON: 87.79 (86.19±104.8)	10.289, 3	0.016*	CON: 10.80	CON vs RSV: >0.999
	RSV: 81.65 (76.40±108.2)			RSV: 7.21	CON vs VPA: 0.313
	VPA: 275.0 (153.4±336.0)			VPA: 18.50	CON vs RSV+VPA: >0.999
	RSV+VPA: 87.05 (66.13±98.72)			RSV+VPA: 7.88	RSV vs VPA: 0.014*
					VPA vs RSV+VPA: 0.066#

II/III: upper cortical layers; **IV/V**: deeper cortical layers; **aCC**: anterior cingulate cortex; **AmR**: amygdala region; **CP**: choroid plexus; **HIP**: hippocampus; **IL**: infralimbic cortex; **IQR**: interquartile range; **PrL**: prelimbic cortex; **pSSA**: primary somatosensory area. p <0.05 was considered significant. *p<0.05, **p<0.01. Statistical analyses: Kruskal-Wallis. N_{CON}: 5, N_{RSV}: 7, N_{VPA}: 4, N_{RSV+VPA}: 4.

Accepted Article

Table 3 – Descriptive statistics of the AQP1 and AQP4 distribution profile in pSSA

	Mean ± SD	F (DFn, DFd); p Value	Pairwise comparisons
AQP1 (II/III)	CON: 438.3±105.9	Interaction: F (1, 17) = 0,013; p = 0.909 VPA: F (1, 17) = 2,171; p = 0.158 RSV: F (1, 17) = 0,064; p = 0.804	CON vs RSV: >0.999
	RSV: 455.8±121.3		CON vs VPA: 0.934
	VPA: 373.7±89.17		CON vs RSV+VPA: 0.966
	RSV+VPA: 380.2±111.2		RSV vs VPA: 0.744
			RSV vs RSV+VPA: 0.838
		VPA vs RSV+VPA: >0.999	
AQP1 (IV/V)	CON: 556.3±140.8	Interaction: F (1, 17) = 0.821; p = 0.377 VPA: F (1, 17) = 18.28; p = 0.0005*** RSV: F (1, 17) = 0.0607; p = 0.808	CON vs RSV: 0.969
	RSV: 507.6±82.91		CON vs VPA: 0.015*
	VPA: 337.6±80.89		CON vs RSV+VPA: 0.049*
	RSV+VPA: 365.4±83.67		RSV vs VPA: 0.039*
			RSV vs RSV+VPA: 0.139
		VPA vs RSV+VPA: 0.997	
AQP4 (II/III)	CON: 154.1±32.47	Interaction: F (1, 18) = 0.6649; p = 0.4255 VPA: F (1, 18) = 0.8502; p = 0.3687 RSV: F (1, 18) = 0.8440; p = 0.3704	CON vs RSV: 0.801
	RSV: 194.3±55.26		CON vs VPA: 0.799
	VPA: 194.4±52.50		CON vs RSV+VPA: 0.789
	RSV+VPA: 196.8±69.81		RSV vs VPA: >0.999
			RSV vs RSV+VPA: >0.999
		VPA vs RSV+VPA: >0.999	
AQP4 (IV/V)	CON: 109.9±23.35	Interaction: F (1, 19) = 14.75; p = 0.0011** VPA: F (1, 19) = 2.573; p = 0.1252 RSV: F (1, 19) = 0.7357; p = 0.4017	CON vs RSV: 0.2348
	RSV: 147.5±21.48		CON vs VPA: 0.0052**
	VPA: 173.8±27.00		CON vs RSV+VPA: 0.9966
	RSV+VPA: 123.7±28.31		RSV vs VPA: 0.4338
			RSV vs RSV+VPA: 0.5920
		VPA vs RSV+VPA: 0.0252*	

II/III: upper cortical layers; **IV/V:** deeper cortical layers; **pSSA:** primary somatosensory area; **SD:** standard deviation. p <0.05 was considered significant. *p<0.05, **p<0.01, ***p<0.001. Statistical analyses: two-way ANOVA parametric test followed by Sidak. N_{CON}: 5, N_{RSV}: 6, N_{VPA}: 6, N_{RSV+VPA}: 5. “Mean” represents de mean of fluorescence.

Table 4 – Descriptive statistics of the AQP1 and AQP4 distribution profile in mPFC

Mean ± SD		F (DFn, DFd); p Value	Pairwise comparisons	
AQP1 aCC (II/III)	CON: 340.0±20.61	Interaction: F (1, 14) = 0.232; p = 0.637 VPA: F (1, 14) = 11.59; p = 0.0043** RSV: F (1, 14) = 0.136 ; p = 0.717	CON vs RSV:	0.989
	RSV: 317.6±59.90		CON vs VPA:	0.091#
	VPA: 237.3±34.16		CON vs RSV+VPA:	0.105
	RSV+VPA: 240.3±89.26		RSV vs VPA:	0.264
			RSV vs RSV+VPA:	0.301
			VPA vs RSV+VPA:	>0.999
AQP1 aCC (IV/V)	CON: 413.4±89.15	Interaction: F (1, 14) = 0.839; p = 0.375 VPA: F (1, 14) = 17.29; p = 0.0010*** RSV: F (1, 14) = 0.0311; p = 0.863	CON vs RSV:	0.995
	RSV: 384.2±68.89		CON vs VPA:	0.017*
	VPA: 213.5±60.90		CON vs RSV+VPA:	0.079#
	RSV+VPA: 256.6±107.4		RSV vs VPA:	0.049*
			RSV vs RSV+VPA:	0.207
			VPA vs RSV+VPA:	0.979
AQP1 PrL (II/III)	CON: 440.8±84.40	Interaction: F (1, 14) = 0.512; p = 0.486 VPA: F (1, 14) = 17.01; p = 0.0010** RSV: F (1, 14) = 0.039; p = 0.845	CON vs RSV:	0.985
	RSV: 400.3±110.8		CON vs VPA:	0.024*
	VPA: 226.7±39.04		CON vs RSV+VPA:	0.050#
	RSV+VPA: 249.5±114.8		RSV vs VPA:	0.086#
			RSV vs RSV+VPA:	0.168
			VPA vs RSV+VPA:	0.999
AQP1 PrL (IV/V)	CON: 444.4±79.13	Interaction: F (1, 14) = 0.028; p = 0.869 VPA: F (1, 14) = 30.04; p < 0.0001**** RSV: F (1, 14) = 3.832; p = 0.0705	CON vs RSV:	0.739
	RSV: 383.0±66.96		CON vs VPA:	0.013*
	VPA: 262.1±52.99		CON vs RSV+VPA:	0.0007***
	RSV+VPA: 189.3±85.19		RSV vs VPA:	0.146
			RSV vs RSV+VPA:	0.0080**
			VPA vs RSV+VPA:	0.686
AQP1 IL (II/III)	CON: 438.1±84.61	Interaction: F (1, 14) = 1.550; p = 0.2336 VPA: F (1, 14) = 17.51; p = 0.0009*** RSV: F (1, 14) = 0.2064 ; p = 0.6565	CON vs RSV:	0.780
	RSV: 365.1±95.19		CON vs VPA:	0.0108*
	VPA: 205.0±41.25		CON vs RSV+VPA:	0.0324*
	RSV+VPA: 238.9±122.0		RSV vs VPA:	0.111
			RSV vs RSV+VPA:	0.294
			VPA vs RSV+VPA:	0.996
AQP1 IL (IV/V)	CON: 459.4±80.84	Interaction: F (1, 14) = 0.069; p = 0.796 VPA: F (1, 14) = 21.20; p = 0.0004*** RSV: F (1, 14) = 0.459; p = 0.5089	CON vs RSV:	0.982
	RSV: 418.4±89.54		CON vs VPA:	0.0236*
	VPA: 247.2±30.44		CON vs RSV+VPA:	0.0132*
	RSV+VPA: 229.1±138.2		RSV vs VPA:	0.086#
			RSV vs RSV+VPA:	0.0489*
			VPA vs RSV+VPA:	>0.999
AQP4 aCC (II/III)	CON: 522.8±86.07	Interaction: F (1, 16) = 4.879; p = 0.0421* VPA: F (1, 16) = 2.709; p = 0.1193 RSV: F (1, 16) = 0.01204; p = 0.9140	CON vs RSV:	0.586
	RSV: 400.5±94.07		CON vs VPA:	0.064#
	VPA: 298.3±119.1		CON vs RSV+VPA:	0.880
	RSV+VPA: 433.3±213.3		RSV vs VPA:	0.787
			RSV vs RSV+VPA:	0.999
			VPA vs RSV+VPA:	0.589
AQP4 aCC (IV/V)	CON: 555.4±160.3	Interaction: F (1, 16) = 7.910; p = 0.0125* VPA: F (1, 16) = 6.711; p = 0.0197* RSV: F (1, 16) = 0.6246 ; p = 0.4409	CON vs RSV:	0.093
	RSV: 354.4±76.63		CON vs VPA:	0.0058**
	VPA: 254.0±42.98		CON vs RSV+VPA:	0.172
	RSV+VPA: 366.8±167.8		RSV vs VPA:	0.769
			RSV vs RSV+VPA:	>0.999
			VPA vs RSV+VPA:	0.722
AQP4 PrL (II/III)	CON: 428.0±68.79	Interaction: F (1, 16) = 4.736; p = 0.0449* VPA: F (1, 16) = 9.964; p = 0.0061** RSV: F (1, 16) = 0.1171 ; p = 0.7367	CON vs RSV:	0.717
	RSV: 354.1±90.40		CON vs VPA:	0.0064**
	VPA: 213.2±45.47		CON vs RSV+VPA:	0.337
	RSV+VPA: 314.6±144.4		RSV vs VPA:	0.134
			RSV vs RSV+VPA:	0.987
			VPA vs RSV+VPA:	0.500

AQP4	CON: 482.0±107.3	Interaction: F (1, 16) = 7.142; p = 0.0167*	CON vs RSV:	0.216
	RSV: 339.8±92.58		CON vs VPA:	0.0061**
PrL	VPA: 227.3±49.74	VPA: F (1, 16) = 7.278; p = 0.0158*	CON vs RSV+VPA:	0.266
	RSV+VPA: 338.6±157.5	RSV: F (1, 16) = 0.1057 ; p = 0.7493	RSV vs VPA:	0.501
(IV/V)			RSV vs RSV+VPA:	>0.999
			VPA vs RSV+VPA:	0.576
AQP4	CON: 466.8±100.4	Interaction: F (1, 16) = 4.930; p = 0.0412*	CON vs RSV:	0.331
	RSV: 356.7±105.0		CON vs VPA:	0.0009***
IL	VPA: 193.8±27.21	VPA: F (1, 16) = 19.05; p = 0.0005***	CON vs RSV+VPA:	0.0237*
	RSV+VPA: 267.8±111.5	RSV: F (1, 16) = 0.1895 ; p = 0.6692	RSV vs VPA:	0.0736#
(II/III)			RSV vs RSV+VPA:	0.668
			VPA vs RSV+VPA:	0.817
AQP4	CON: 446.3±70.78	Interaction: F (1, 16) = 7.073; p = 0.0171*	CON vs RSV:	0.184
	RSV: 333.9±87.51		CON vs VPA:	0.0029**
IL	VPA: 235.7±52.18	VPA: F (1, 16) = 10.13; p = 0.0058**	CON vs RSV+VPA:	0.122
	RSV+VPA: 315.0±108.4	RSV: F (1, 16) = 0.2106 ; p = 0.6525	RSV vs VPA:	0.351
(IV/V)			RSV vs RSV+VPA:	0.999
			VPA vs RSV+VPA:	0.643

II/III: upper cortical layers; **IV/V**: deeper cortical layers; **aCC**: anterior cingulate cortex; **IL**: infralimbic cortex; **PrL**: prelimbic cortex; **SD**: standard deviation. p <0.05 was considered significant. *p<0.05, **p<0.01, ***p<0.001, ****p<0.0001. Statistical analyses: two-way ANOVA parametric test followed by Sidak. N_{CON}: 5, N_{RSV}: 6, N_{VPA}: 6, N_{RSV+VPA}: 5. “Mean” represents de mean of fluorescence.

Table 5 – Descriptive statistics of the AQP1 and AQP4 distribution profile in AmR

	Mean ± SD	F (DFn, DFd); p Value	Pairwise comparisons	
AQP1	CON: 394.4±13.92	Interaction: F (1, 17) = 0.0279; p = 0.869 VPA: F (1, 17) = 18.95; p = 0.0004*** RSV: F (1, 17) = 3.226; p = 0.090	CON vs RSV:	0.8603
	RSV: 354.3±46.69		CON vs VPA:	0.0621#
	VPA: 291.2±67.83		CON vs RSV+VPA:	0.0049**
	RSV+VPA: 242.8±67.61		RSV vs VPA:	0.3386
		RSV vs RSV+VPA:	0.0249*	
		VPA vs RSV+VPA:	0.6718	
AQP4	CON: 112.9±15.93	Interaction: F (1, 16) = 0.2881; p = 0.5988 VPA: F (1, 16) = 0.1118; p = 0.7425 RSV: F (1, 16) = 0.9222; p = 0.3512	CON vs RSV:	0.887
	RSV: 124.6±11.77		CON vs VPA:	0.991
	VPA: 119.7±10.60		CON vs RSV+VPA:	0.939
	RSV+VPA: 123.0±26.89		RSV vs VPA:	0.998
			RSV vs RSV+VPA:	>0.999
		VPA vs RSV+VPA:	0.999	

AmR: amygdala region; **SD:** standard deviation. p <0.05 was considered significant. *p<0.05, **p<0.01, ***p<0.001. Statistical analyses: two-way ANOVA parametric test followed by Sidak. N_{CON}: 5, N_{RSV}: 6, N_{VPA}: 6, N_{RSV+VPA}: 5. “Mean” represents de mean of fluorescence.

Accepted Article

Table 6 – Descriptive statistics of the AQP1 and AQP4 distribution profile in hippocampus.

Mean ± SD		F (DFn, DFd); p Value	Pairwise comparisons	
AQP1 DG	CON: 420.2±68.76 RSV: 315.9±121.7 VPA: 387.9±154.8 RSV+VPA: 260.1±123.2	Interaction: F (1, 18) = 0.049; p = 0.826 VPA: F (1, 18) = 0.697; p = 0.415 RSV: F (1, 18) = 4.837; p = 0.041*	CON vs RSV: 0.694 CON vs VPA: 0.999 CON vs RSV+VPA: 0.287 RSV vs VPA: 0.905 RSV vs RSV+VPA: 0.976 VPA vs RSV+VPA: 0.482	
			CON vs RSV: 0.607 CON vs VPA: 0.841 CON vs RSV+VPA: 0.136 RSV vs VPA: 0.999 RSV vs RSV+VPA: 0.892 VPA vs RSV+VPA: 0.679	
AQP1 CA1	CON: 418.9±72.71 RSV: 316.8±114.7 VPA: 341.8±107.7 RSV+VPA: 246.9±136.7	Interaction: F (1, 18) = 0.0057; p = 0.940 VPA: F (1, 18) = 2.413; p = 0.137 RSV: F (1, 18) = 4.340; p = 0.052#	CON vs RSV: 0.768 CON vs VPA: 0.895 CON vs RSV+VPA: 0.057 RSV vs VPA: >0.999 RSV vs RSV+VPA: 0.465 VPA vs RSV+VPA: 0.327	
			CON vs RSV: 0.972 CON vs VPA: 0.997 CON vs RSV+VPA: 0.212 RSV vs VPA: 0.999 RSV vs RSV+VPA: 0.592 VPA vs RSV+VPA: 0.404	
AQP1 CA2	CON: 424.1±50.26 RSV: 340.3±107.3 VPA: 356.3±126.8 RSV+VPA: 226.6±124.3	Interaction: F (1, 18) = 0.245; p = 0.626 VPA: F (1, 18) = 3.858; p = 0.065 RSV: F (1, 18) = 5.331; p = 0.033*	CON vs RSV: 0.967 CON vs VPA: 0.718 CON vs RSV+VPA: 0.929 RSV vs VPA: 0.997 RSV vs RSV+VPA: 0.437 VPA vs RSV+VPA: 0.135	
			CON vs RSV: 0.935 CON vs VPA: 0.929 CON vs RSV+VPA: 0.982 RSV vs VPA: >0.999 RSV vs RSV+VPA: 0.505 VPA vs RSV+VPA: 0.447	
AQP1 CA3	CON: 366.6±54.55 RSV: 316.9±105.5 VPA: 335.5±120.2 RSV+VPA: 217.8±124.0	Interaction: F (1, 18) = 0.564; p = 0.462 VPA: F (1, 18) = 2.071; p = 0.167 RSV: F (1, 18) = 3.418; p = 0.081#	CON vs RSV: 0.901 CON vs VPA: 0.979 CON vs RSV+VPA: 0.995 RSV vs VPA: 0.999 RSV vs RSV+VPA: 0.540 VPA vs RSV+VPA: 0.717	
			CON vs RSV: 0.353 CON vs VPA: 0.967 CON vs RSV+VPA: >0.999 RSV vs VPA: 0.770 RSV vs RSV+VPA: 0.238 VPA vs RSV+VPA: 0.909	
AQP4 DG	CON: 297.6±56.51 RSV: 338.4±50.03 VPA: 361.9±96.46 RSV+VPA: 251.4±95.38	Interaction: F (1, 19) = 4.936; p = 0.0387* VPA: F (1, 19) = 0.1120; p = 0.7415 RSV: F (1, 19) = 1.048; p = 0.3187		
AQP4 CA1	CON: 300.7±44.61 RSV: 346.4±66.26 VPA: 343.9±107.4 RSV+VPA: 267.2±65.51	Interaction: F (1, 19) = 3.456; p = 0.0786# VPA: F (1, 19) = 0.2992; p = 0.5908 RSV: F (1, 19) = 0.2202; p = 0.6442		
AQP4 CA2	CON: 307.7±73.17 RSV: 351.1±40.68 VPA: 336.3±79.70 RSV+VPA: 285.2±62.61	Interaction: F (1, 19) = 2.790; p = 0.1113 VPA: F (1, 19) = 0.4353; p = 0.5173 RSV: F (1, 19) = 0.01884; p = 0.8923		
AQP4 CA3	CON: 277.4±48.82 RSV: 342.3±27.86 VPA: 302.4±68.88 RSV+VPA: 272.6±51.07	Interaction: F (1, 19) = 4.422; p = 0.0490* VPA: F (1, 19) = 0.9866; p = 0.3331 RSV: F (1, 19) = 0.6090; p = 0.4448		

DG: dentate gyrus; **SD:** standard deviation. p <0.05 was considered significant. *p<0.05. Statistical analyses: two-way ANOVA parametric test followed by Sidak. N_{CON}: 5, N_{RSV}: 6, N_{VPA}: 6, N_{RSV+VPA}: 5. “Mean” represents de mean of fluorescence.

Table 7 – Descriptive statistics of the GFAP fluorescence and number of GFAP⁺-astrocytes in pSSA

	Mean ± SD	F (DFn, DFd); p Value	Pairwise comparisons
GFAP (II/III)	CON: 153.1±38.39	Interaction: F (1, 18) = 0.1940; p = 0.6649 VPA: F (1, 18) = 5.797; p = 0.0270* RSV: F (1, 18) = 2.023; p = 0.1721	CON vs RSV: 0.983
	RSV: 177.3±49.76		CON vs VPA: 0.6985
	VPA: 201.6±35.43		CON vs RSV+VPA: 0.105
	RSV+VPA: 247.4±93.58		RSV vs VPA: 0.978
			RSV vs RSV+VPA: 0.306
		VPA vs RSV+VPA: 0.746	
GFAP (IV/V)	CON: 109.6±45.17	Interaction: F (1, 18) = 0.3125; p = 0.5831 VPA: F (1, 18) = 2.004; p = 0.1740 RSV: F (1, 18) = 5.017; p = 0.0380*	CON vs RSV: 0.822
	RSV: 146.5±32.95		CON vs VPA: 0.991
	VPA: 128.4±8.990		CON vs RSV+VPA: 0.133
	RSV+VPA: 189.9±91.40		RSV vs VPA: 0.991
			RSV vs RSV+VPA: 0.695
		VPA vs RSV+VPA: 0.324	
Number (II/III)	CON: 66.40±19.51	Interaction: F (1, 18) = 0.7098; p = 0.4106 VPA: F (1, 18) = 10.99; p = 0.0038** RSV: F (1, 18) = 0.4752; p = 0.4994	CON vs RSV: >0.999
	RSV: 65.00±28.09		CON vs VPA: 0.459
	VPA: 89.00±22.12		CON vs RSV+VPA: 0.082#
	RSV+VPA: 103.0±8.485		RSV vs VPA: 0.341
			RSV vs RSV+VPA: 0.051#
		VPA vs RSV+VPA: 0.875	
Number (IV/V)	CON: 39.40±18.42	Interaction: F (1, 18) = 0.4240; p = 0.5232 VPA: F (1, 18) = 11.05; p = 0.0038** RSV: F (1, 18) = 4.086; p = 0.0584#	CON vs RSV: 0.373
	RSV: 63.00±18.45		CON vs VPA: 0.067#
	VPA: 74.50±28.47		CON vs RSV+VPA: 0.0117*
	RSV+VPA: 86.60±11.67		RSV vs VPA: 0.922
			RSV vs RSV+VPA: 0.373
		VPA vs RSV+VPA: 0.921	

II/III: upper cortical layers; **IV/V:** deeper cortical layers; **pSSA:** primary somatosensory area; **SD:** standard deviation. p <0.05 was considered significant. *p<0.05, **p<0.01. Statistical analyses: two-way ANOVA parametric test followed by Sidak. N_{CON}: 5, N_{RSV}: 6, N_{VPA}: 6, N_{RSV+VPA}: 5.

Table 8 – Descriptive statistics of the GFAP fluorescence and number of GFAP⁺-astrocytes in mPFC

		Mean ± SD	F (DFn, DFd); p Value	Pairwise comparisons	
GFAP	CON:	316.5±48.96	Interaction: F (1, 14) = 2.882; p = 0.1117	CON vs RSV:	0.980
	RSV:	366.6±87.41		CON vs VPA:	0.0789#
aCC (II/III)	VPA:	522.5±157.7	VPA: F (1, 14) = 5.252; p = 0.0379*	CON vs RSV+VPA:	0.869
	RSV+VPA:	397.2±130.6	RSV: F (1, 14) = 0.5305; p = 0.4784	RSV vs VPA:	0.269
				RSV vs RSV+VPA:	0.998
				VPA vs RSV+VPA:	0.554
GFAP	CON:	307.0±30.66	Interaction: F (1, 14) = 7.310; p = 0.0171*	CON vs RSV:	0.999
	RSV:	319.9±44.57		CON vs VPA:	0.0348*
aCC (IV/V)	VPA:	422.3±49.83	VPA: F (1, 14) = 3.549; p = 0.0805	CON vs RSV+VPA:	>0.999
	RSV+VPA:	299.3±81.86	RSV: F (1, 14) = 4.806; p = 0.0458*	RSV vs VPA:	0.071#
				RSV vs RSV+VPA:	0.993
				VPA vs RSV+VPA:	0.0321*
GFAP	CON:	297.9±35.88	Interaction: F (1, 14) = 1.234; p = 0.2853	CON vs RSV:	0.999
	RSV:	313.1±61.58		CON vs VPA:	0.231
PrL (II/III)	VPA:	406.1±79.69	VPA: F (1, 14) = 4.171; p = 0.0604#	CON vs RSV+VPA:	0.923
	RSV+VPA:	345.0±106.4	RSV: F (1, 14) = 0.4471; p = 0.5146	RSV vs VPA:	0.377
				RSV vs RSV+VPA:	0.987
				VPA vs RSV+VPA:	0.825
GFAP	CON:	312.7±31.30	Interaction: F (1, 14) = 4.820; p = 0.0455*	CON vs RSV:	0.979
	RSV:	288.5±44.65		CON vs VPA:	0.061#
PrL (IV/V)	VPA:	416.3±48.23	VPA: F (1, 14) = 3.930; p = 0.0674#	CON vs RSV+VPA:	0.960
	RSV+VPA:	283.2±80.47	RSV: F (1, 14) = 10.05; p = 0.0068**	RSV vs VPA:	0.0158*
				RSV vs RSV+VPA:	>0.999
				VPA vs RSV+VPA:	0.0173*
GFAP	CON:	338.2±49.43	Interaction: F (1, 14) = 0.3527; p = 0.5621	CON vs RSV:	0.955
	RSV:	297.2±55.84		CON vs VPA:	0.746
IL (II/III)	VPA:	405.2±106.1	VPA: F (1, 14) = 1.659; p = 0.2186	CON vs RSV+VPA:	0.999
	RSV+VPA:	322.0±87.58	RSV: F (1, 14) = 3.036; p = 0.1034	RSV vs VPA:	0.265
				RSV vs RSV+VPA:	0.997
				VPA vs RSV+VPA:	0.593
GFAP	CON:	316.5±24.27	Interaction: F (1, 14) = 2.159; p = 0.1638	CON vs RSV:	0.723
	RSV:	270.5±60.38		CON vs VPA:	0.204
IL (IV/V)	VPA:	398.6±70.81	VPA: F (1, 14) = 3.182; p = 0.0962#	CON vs RSV+VPA:	0.886
	RSV+VPA:	278.4±50.56	RSV: F (1, 14) = 10.84; p = 0.0053**	RSV vs VPA:	0.0176*
				RSV vs RSV+VPA:	>0.999
				VPA vs RSV+VPA:	0.0383*
Number	CON:	109.2±25.58	Interaction: F (1, 15) = 0.04255; p = 0.8393	CON vs RSV:	0.869
	RSV:	139.8±61.92		CON vs VPA:	0.240
aCC (II/III)	VPA:	170.0±22.97	VPA: F (1, 15) = 7.828; p = 0.0135*	CON vs RSV+VPA:	0.075
	RSV+VPA:	192.3±54.32	RSV: F (1, 15) = 1.705; p = 0.2113	RSV vs VPA:	0.876
				RSV vs RSV+VPA:	0.451
				VPA vs RSV+VPA:	0.975
Number	CON:	85.00±21.71	Interaction: F (1, 15) = 1.542; p = 0.2334	CON vs RSV:	0.897
	RSV:	113.6±48.03		CON vs VPA:	0.0443*
aCC (IV/V)	VPA:	170.0±25.50	VPA: F (1, 15) = 8.959; p = 0.0091**	CON vs RSV+VPA:	0.243
	RSV+VPA:	148.8±70.04	RSV: F (1, 15) = 0.033; p = 0.8572	RSV vs VPA:	0.303
				RSV vs RSV+VPA:	0.818
				VPA vs RSV+VPA:	0.979
Number	CON:	111.4±45.53	Interaction: F (1, 15) = 0.4302; p = 0.5218	CON vs RSV:	>0.999
	RSV:	114.0±54.61		CON vs VPA:	0.756
PrL (II/III)	VPA:	156.2±30.54	VPA: F (1, 15) = 6.018; p = 0.0269*	CON vs RSV+VPA:	0.232
	RSV+VPA:	191.5±81.46	RSV: F (1, 15) = 0.5779; p = 0.4589	RSV vs VPA:	0.801
				RSV vs RSV+VPA:	0.262
				VPA vs RSV+VPA:	0.921

Number	CON: 93.20±19.65	Interaction: F (1, 15) = 0.291; p = 0.5978	CON vs RSV:	0.998
	RSV: 105.0±39.21		CON vs VPA:	0.0120*
PrL (IV/V)	VPA: 188.2±21.46	VPA: F (1, 15) = 20.99; p = 0.0004***	CON vs RSV+VPA:	0.0342*
	RSV+VPA: 180.0±70.15	RSV: F (1, 15) = 0.010; p = 0.9240	RSV vs VPA:	0.0307*
			RSV vs RSV+VPA:	0.081#
			VPA vs RSV+VPA:	0.999
Number	CON: 103.6±31.94	Interaction: F (1, 15) = 0.2208; p = 0.6452	CON vs RSV:	>0.999
	RSV: 106.6±79.16		CON vs VPA:	0.678
IL (II/III)	VPA: 158.0±49.46	VPA: F (1, 15) = 5.935; p = 0.0278*	CON vs RSV+VPA:	0.292
	RSV+VPA: 187.0±70.94	RSV: F (1, 15) = 0.3345; p = 0.5716	RSV vs VPA:	0.729
			RSV vs RSV+VPA:	0.328
			VPA vs RSV+VPA:	0.980
Number	CON: 82.20±33.26	Interaction: : F (1, 15) = 4.55e-005; p = 0.9947	CON vs RSV:	>0.999
	RSV: 89.00±36.88		CON vs VPA:	0.084#
IL (IV/V)	VPA: 166.4±50.58	VPA: F (1, 15) = 14.41; p = 0.0018**	CON vs RSV+VPA:	0.074#
	RSV+VPA: 173.5±70.11	RSV: F (1, 15) = 0.097; p = 0.7587	RSV vs VPA:	0.128
			RSV vs RSV+VPA:	0.118
			VPA vs RSV+VPA:	>0.999

II/III: upper cortical layers; **IV/V**: deeper cortical layers; **aCC**: anterior cingulate cortex; **IL**: infralimbic cortex; **PrL**: prelimbic cortex; **SD**: standard deviation. p <0.05 was considered significant. *p<0.05, **p<0.01, ***p<0.001. Statistical analyses: two-way ANOVA parametric test followed by Sidak. N_{CON}: 5, N_{RSV}: 6, N_{VPA}: 6, N_{RSV+VPA}: 5.

Table 9 – Descriptive statistics of the GFAP fluorescence and number of GFAP⁺-astrocytes in AmR

	Mean ± SD	F (DFn, DFd); p Value	Pairwise comparisons
GFAP	CON: 88.98±30.23	Interaction: F (1, 16) = 4.728; p = 0.0450* VPA: F (1, 16) = 3.357; p = 0.0856 RSV: F (1, 16) = 2.095; p = 0.1670	CON vs RSV: 0.996
	RSV: 75.56±14.83		CON vs VPA: >0.999
	VPA: 82.66±14.10		CON vs RSV+VPA: 0.187
	RSV+VPA: 149.6±74.12		RSV vs VPA: >0.999
			RSV vs RSV+VPA: 0.069#
Number	CON: 33.80±7.463	Interaction: F (1, 16) = 14.26; p = 0.0017** VPA: F (1, 16) = 1.307; p = 0.2697 RSV: F (1, 16) = 0.01080; p = 0.9185	VPA vs RSV+VPA: 0.119
	RSV: 11.40±5.225		CON vs RSV: 0.083#
	VPA: 18.60±10.53		CON vs VPA: 0.398
	RSV+VPA: 39.80±21.74		CON vs RSV+VPA: 0.978
			RSV vs VPA: 0.948
		RSV vs RSV+VPA: 0.0185*	
		VPA vs RSV+VPA: 0.111	

AmR: amygdala region; **SD:** standard deviation. p <0.05 was considered significant. *p<0.05, **p<0.01. Statistical analyses: two-way ANOVA parametric test followed by Sidak. N_{CON}: 5, N_{RSV}: 6, N_{VPA}: 6, N_{RSV+VPA}: 5.

Accepted Article

Table 10 – Descriptive statistics of the GFAP fluorescence and number of GFAP⁺-astrocytes in hippocampus.

		Mean ± SD	F (DFn, DFd); p Value	Pairwise comparisons	
GFAP	DG	CON: 458.6±93.64	Interaction: F (1, 19) = 8.292; p = 0.0096** VPA: F (1, 19) = 1.130; p = 0.3012 RSV: F (1, 19) = 0.3929; p = 0.5382	CON vs RSV:	0.170
		RSV: 642.1±62.81		CON vs VPA:	0.751
GFAP	CA1	VPA: 553.7±135.4	Interaction: F (1, 19) = 6.811; p = 0.0172* VPA: F (1, 19) = 2.175; p = 0.1567 RSV: F (1, 19) = 0.2951; p = 0.5933	CON vs RSV+VPA:	0.999
		RSV+VPA: 435.8±162.8		RSV vs VPA:	0.806
GFAP	CA2	CON: 445.0±121.7	Interaction: F (1, 19) = 6.286; p = 0.0214* VPA: F (1, 19) = 2.539; p = 0.1276 RSV: F (1, 19) = 4.842; p = 0.0403*	RSV vs RSV+VPA:	0.0753#
		RSV: 623.1±140.4		VPA vs RSV+VPA:	0.484
GFAP	CA3	VPA: 509.1±168.7	Interaction: F (1, 19) = 9.676; p = 0.0058** VPA: F (1, 19) = 6.882; p = 0.0167* RSV: F (1, 19) = 11.25; p = 0.0033**	CON vs RSV:	0.262
		RSV+VPA: 392.4±81.06		CON vs VPA:	0.964
GFAP	Number	CON: 409.5±170.2	Interaction: F (1, 19) = 6.965; p = 0.0162* VPA: F (1, 19) = 0.03032; p = 0.8636 RSV: F (1, 19) = 2.353; p = 0.1416	CON vs RSV+VPA:	0.988
		RSV: 635.5±73.25		RSV vs VPA:	0.656
GFAP	DG	VPA: 453.4±109.4	Interaction: F (1, 19) = 1.825; p = 0.1926 VPA: F (1, 19) = 0.04939; p = 0.8265 RSV: F (1, 19) = 2.762; p = 0.1129	RSV vs RSV+VPA:	0.0611#
		RSV+VPA: 438.6±86.79		VPA vs RSV+VPA:	0.578
GFAP	CA1	CON: 427.0±97.55	Interaction: F (1, 19) = 0.4575; p = 0.5069 VPA: F (1, 19) = 0.1254; p = 0.7272 RSV: F (1, 19) = 23.66; p = 0.0001***	CON vs RSV:	0.0323*
		RSV: 682.6±36.56		CON vs VPA:	0.987
GFAP	CA2	VPA: 446.3±119.8	Interaction: F (1, 19) = 4.553; p = 0.0461* VPA: F (1, 19) = 6.695; p = 0.0181* RSV: F (1, 19) = 8.936; p = 0.0075**	CON vs RSV+VPA:	0.998
		RSV+VPA: 455.9±87.03		RSV vs VPA:	0.077#
GFAP	CA3	CON: 80.80±11.73	Interaction: F (1, 19) = 4.553; p = 0.0461* VPA: F (1, 19) = 6.695; p = 0.0181* RSV: F (1, 19) = 8.936; p = 0.0075**	RSV vs RSV+VPA:	0.059#
		RSV: 120.8±28.44		VPA vs RSV+VPA:	>0.999
GFAP	Number	VPA: 104.4±22.65	Interaction: F (1, 19) = 1.825; p = 0.1926 VPA: F (1, 19) = 0.04939; p = 0.8265 RSV: F (1, 19) = 2.762; p = 0.1129	CON vs RSV:	0.0023**
		RSV+VPA: 93.83±24.41		CON vs VPA:	0.999
GFAP	CA1	CON: 71.00±19.25	Interaction: F (1, 19) = 0.4575; p = 0.5069 VPA: F (1, 19) = 0.1254; p = 0.7272 RSV: F (1, 19) = 23.66; p = 0.0001***	CON vs RSV+VPA:	0.996
		RSV: 99.60±29.59		RSV vs VPA:	0.0023**
GFAP	CA2	VPA: 81.71±19.49	Interaction: F (1, 19) = 4.553; p = 0.0461* VPA: F (1, 19) = 6.695; p = 0.0181* RSV: F (1, 19) = 8.936; p = 0.0075**	RSV vs RSV+VPA:	0.0047**
		RSV+VPA: 84.67±21.86		VPA vs RSV+VPA:	>0.999
GFAP	CA3	CON: 76.40±12.40	Interaction: F (1, 19) = 4.553; p = 0.0461* VPA: F (1, 19) = 6.695; p = 0.0181* RSV: F (1, 19) = 8.936; p = 0.0075**	CON vs RSV:	0.069#
		RSV: 118.8±16.63		CON vs VPA:	0.999
GFAP	Number	VPA: 84.29±20.77	Interaction: F (1, 19) = 4.553; p = 0.0461* VPA: F (1, 19) = 6.695; p = 0.0181* RSV: F (1, 19) = 8.936; p = 0.0075**	CON vs RSV+VPA:	0.928
		RSV+VPA: 116.3±19.82		RSV vs VPA:	0.798
GFAP	CA1	CON: 88.20±17.75	Interaction: F (1, 19) = 4.553; p = 0.0461* VPA: F (1, 19) = 6.695; p = 0.0181* RSV: F (1, 19) = 8.936; p = 0.0075**	RSV vs RSV+VPA:	0.333
		RSV: 132.4±18.50		VPA vs RSV+VPA:	0.959
GFAP	CA2	VPA: 84.29±21.88	Interaction: F (1, 19) = 4.553; p = 0.0461* VPA: F (1, 19) = 6.695; p = 0.0181* RSV: F (1, 19) = 8.936; p = 0.0075**	CON vs RSV:	0.307
		RSV+VPA: 91.67±22.23		CON vs VPA:	0.965
GFAP	CA3	CON: 88.20±17.75	Interaction: F (1, 19) = 4.553; p = 0.0461* VPA: F (1, 19) = 6.695; p = 0.0181* RSV: F (1, 19) = 8.936; p = 0.0075**	CON vs RSV+VPA:	0.908
		RSV: 132.4±18.50		RSV vs VPA:	0.720
GFAP	Number	VPA: 84.29±21.88	Interaction: F (1, 19) = 4.553; p = 0.0461* VPA: F (1, 19) = 6.695; p = 0.0181* RSV: F (1, 19) = 8.936; p = 0.0075**	RSV vs RSV+VPA:	0.869
		RSV+VPA: 91.67±22.23		VPA vs RSV+VPA:	>0.999
GFAP	CA1	CON: 88.20±17.75	Interaction: F (1, 19) = 4.553; p = 0.0461* VPA: F (1, 19) = 6.695; p = 0.0181* RSV: F (1, 19) = 8.936; p = 0.0075**	CON vs RSV:	0.0093**
		RSV: 132.4±18.50		CON vs VPA:	0.977
GFAP	CA2	VPA: 84.29±21.88	Interaction: F (1, 19) = 4.553; p = 0.0461* VPA: F (1, 19) = 6.695; p = 0.0181* RSV: F (1, 19) = 8.936; p = 0.0075**	CON vs RSV+VPA:	0.0107*
		RSV+VPA: 91.67±22.23		RSV vs VPA:	0.0253*
GFAP	CA3	CON: 88.20±17.75	Interaction: F (1, 19) = 4.553; p = 0.0461* VPA: F (1, 19) = 6.695; p = 0.0181* RSV: F (1, 19) = 8.936; p = 0.0075**	RSV vs RSV+VPA:	>0.999
		RSV: 132.4±18.50		VPA vs RSV+VPA:	0.0299*
GFAP	Number	VPA: 84.29±21.88	Interaction: F (1, 19) = 4.553; p = 0.0461* VPA: F (1, 19) = 6.695; p = 0.0181* RSV: F (1, 19) = 8.936; p = 0.0075**	CON vs RSV:	0.0174*
		RSV+VPA: 91.67±22.23		CON vs VPA:	0.999
GFAP	CA1	CON: 88.20±17.75	Interaction: F (1, 19) = 4.553; p = 0.0461* VPA: F (1, 19) = 6.695; p = 0.0181* RSV: F (1, 19) = 8.936; p = 0.0075**	CON vs RSV+VPA:	0.999
		RSV: 132.4±18.50		RSV vs VPA:	0.0045**
GFAP	CA2	VPA: 84.29±21.88	Interaction: F (1, 19) = 4.553; p = 0.0461* VPA: F (1, 19) = 6.695; p = 0.0181* RSV: F (1, 19) = 8.936; p = 0.0075**	RSV vs RSV+VPA:	0.0232*
		RSV+VPA: 91.67±22.23		VPA vs RSV+VPA:	0.988

DG: dentate gyrus; **SD:** standard deviation. p <0.05 was considered significant. *p<0.05, **p<0.01, ***p<0.001. Statistical analyses: two-way ANOVA parametric test followed by Sidak. N_{CON}: 5, N_{RSV}: 6, N_{VPA}: 6, N_{RSV+VPA}: 5.